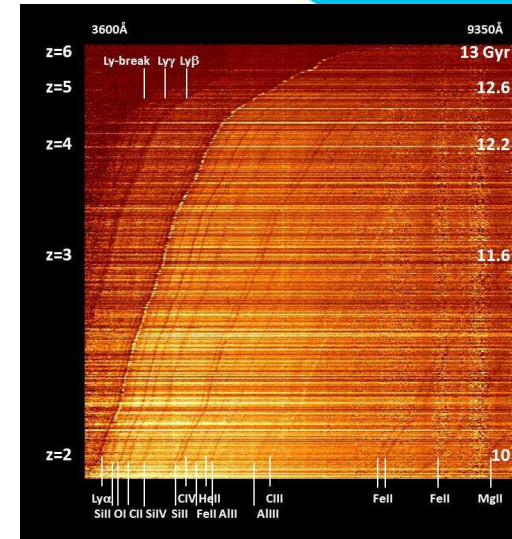


Diagnostic emission lines in the Early Universe

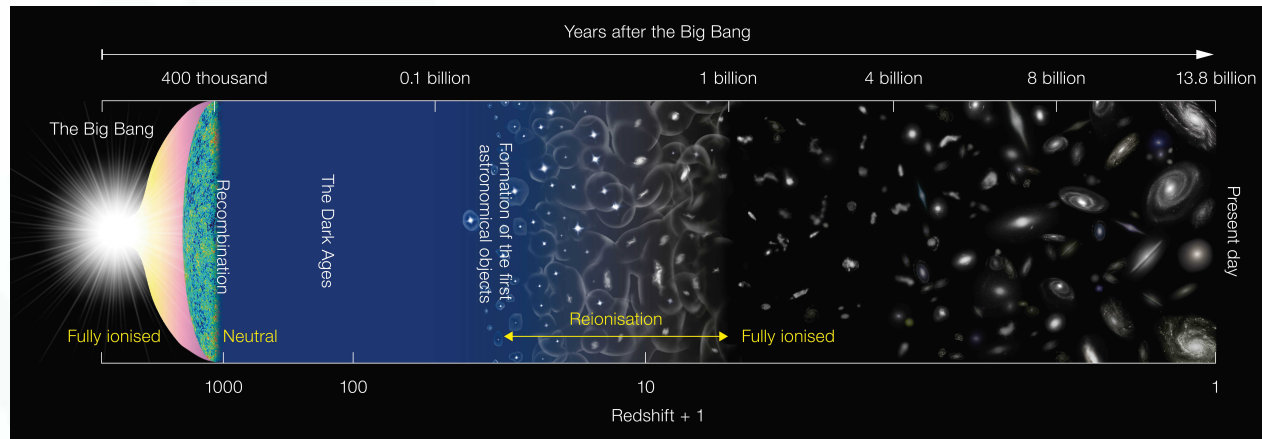


P. Theulé, J. Villa-Vélez, V. Buat, D. Burgarella, M. Boquien
L.M. Seillé, E. Pons, L. Trabelsi, O. Kalpogiannis

Laboratoire d'Astrophysique de Marseille, Aix-Marseille Université
"14th Serbian Conference on Spectral Line Shapes in Astrophysics"
June 19-23, 2023, Bajina Basta, Serbia

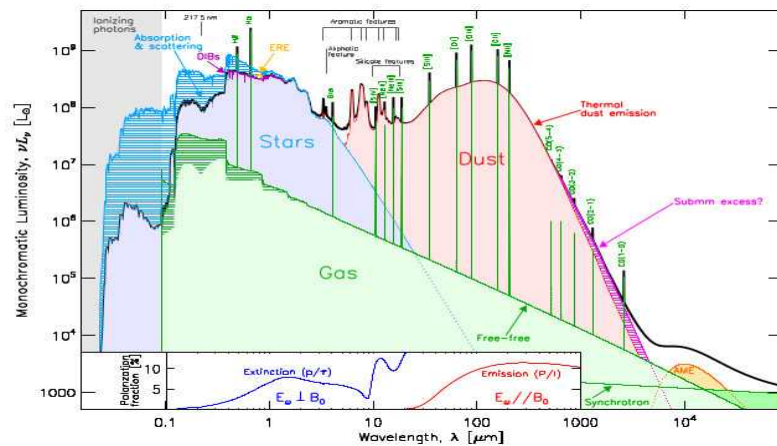
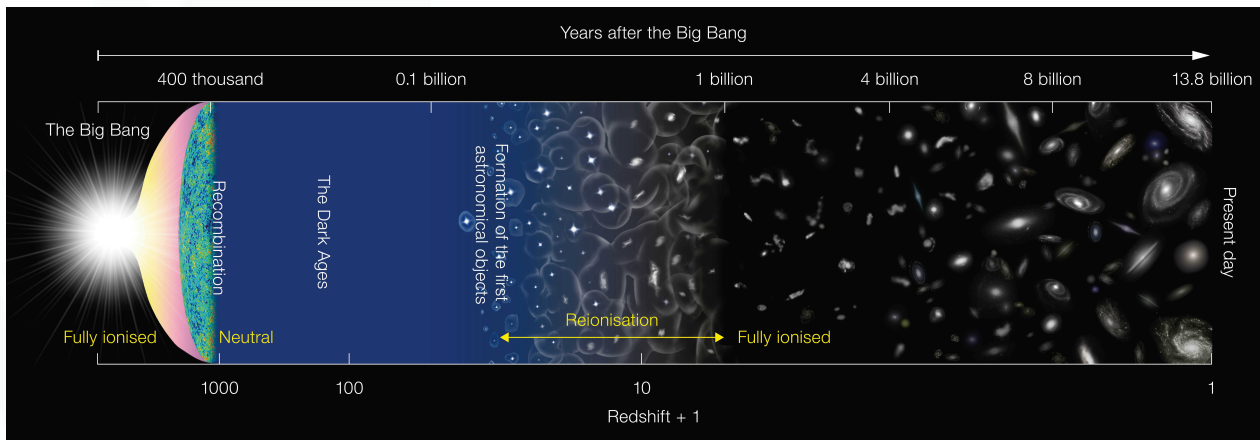
Scientific goals

→ to derive galaxy evolution relevant parameters (star formation history, initial mass function, density, metallicity, cosmic ray, photoradiation field, ...) from the epoch of re-ionization ($6 < z < 25$) to now ($z=0$) from galaxies spectral energy distribution



Scientific goals

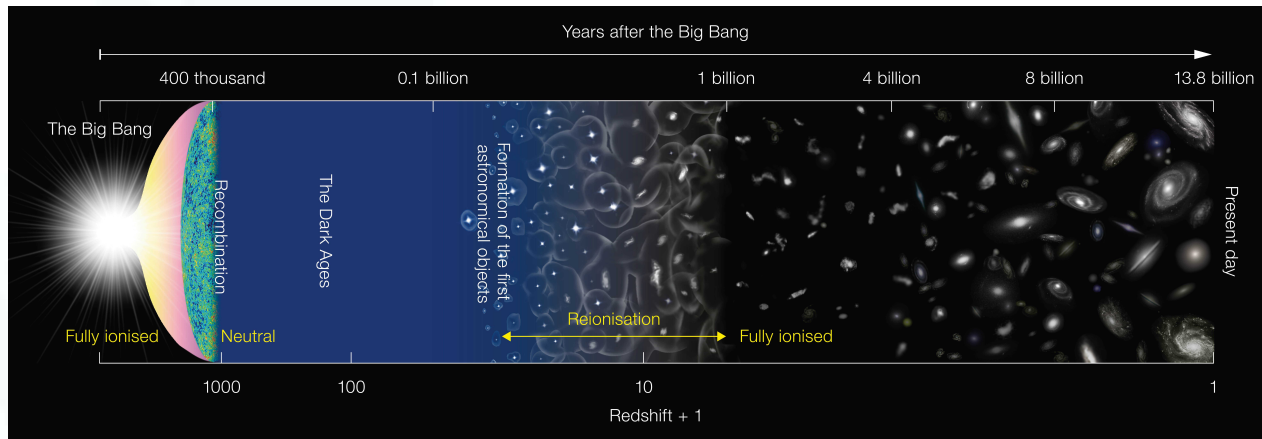
→ to derive galaxy evolution relevant parameters (star formation history, initial mass function, density, metallicity, cosmic ray, photoradiation field, ...) from the epoch of re-ionization ($6 < z < 25$) to now ($z=0$) from galaxies spectral energy distribution



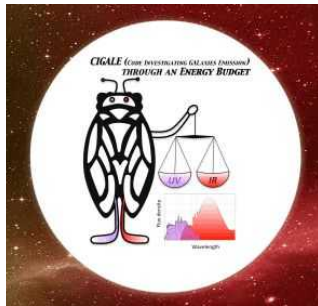
credit : F. Galliano et al. ARAA 2018

Scientific goals

→ to derive galaxy evolution relevant parameters (star formation history, initial mass function, density, metallicity, cosmic ray, photoradiation field, ...) from the epoch of re-ionization ($6 < z < 25$) to now ($z=0$) from galaxies spectral energy distribution



→ to combine spectro- and photometric analysis of galaxies around Cosmic Noon

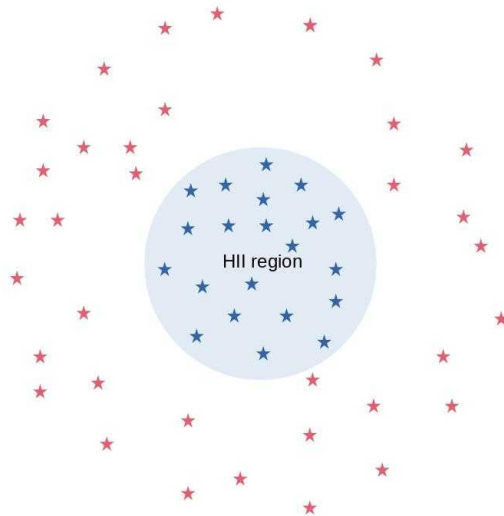


PhD Jorge Villa-Vélez :
Spectro-photometric Analysis Around Cosmic Noon:
Emission-Lines, Dust Attenuation, and Star Formation

Fitting spectral energy distributions of FMOS-COSMOS emission-line galaxies at $z \sim 1.6$:
Star formation rates, dust attenuation, and $[OIII]\lambda 5007$ emission-line luminosities
Villa-Vélez J. A. , Buat V., Theulé P. , Boquien M., Burgarella D.,
Astronomy & Astrophysics, 2021

→ to generate mock spectra for next-coming instruments VLT/MOONS, Subaru/PFS, ELT/Mosaic

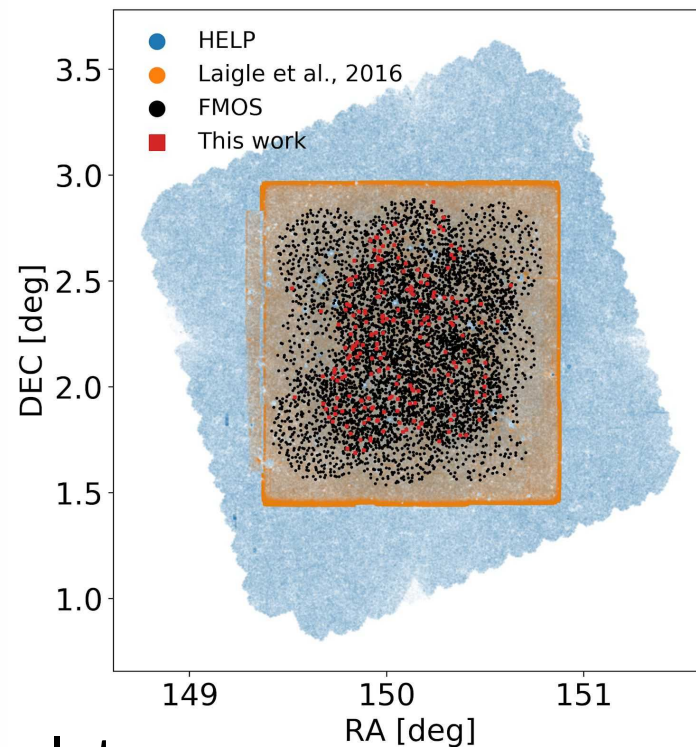
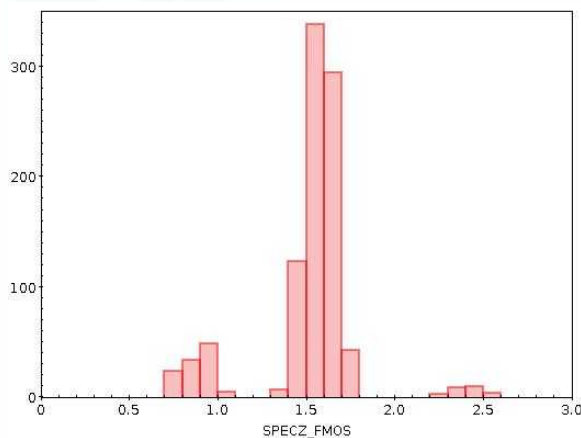
I. Starburst regions



1. Technique validation on a reduced sample with spectroscopic data
2. Extension to a larger sample
3. Updates on CIGALE line fitting capacities improvements

Selection of our COSMOS field sub-sample

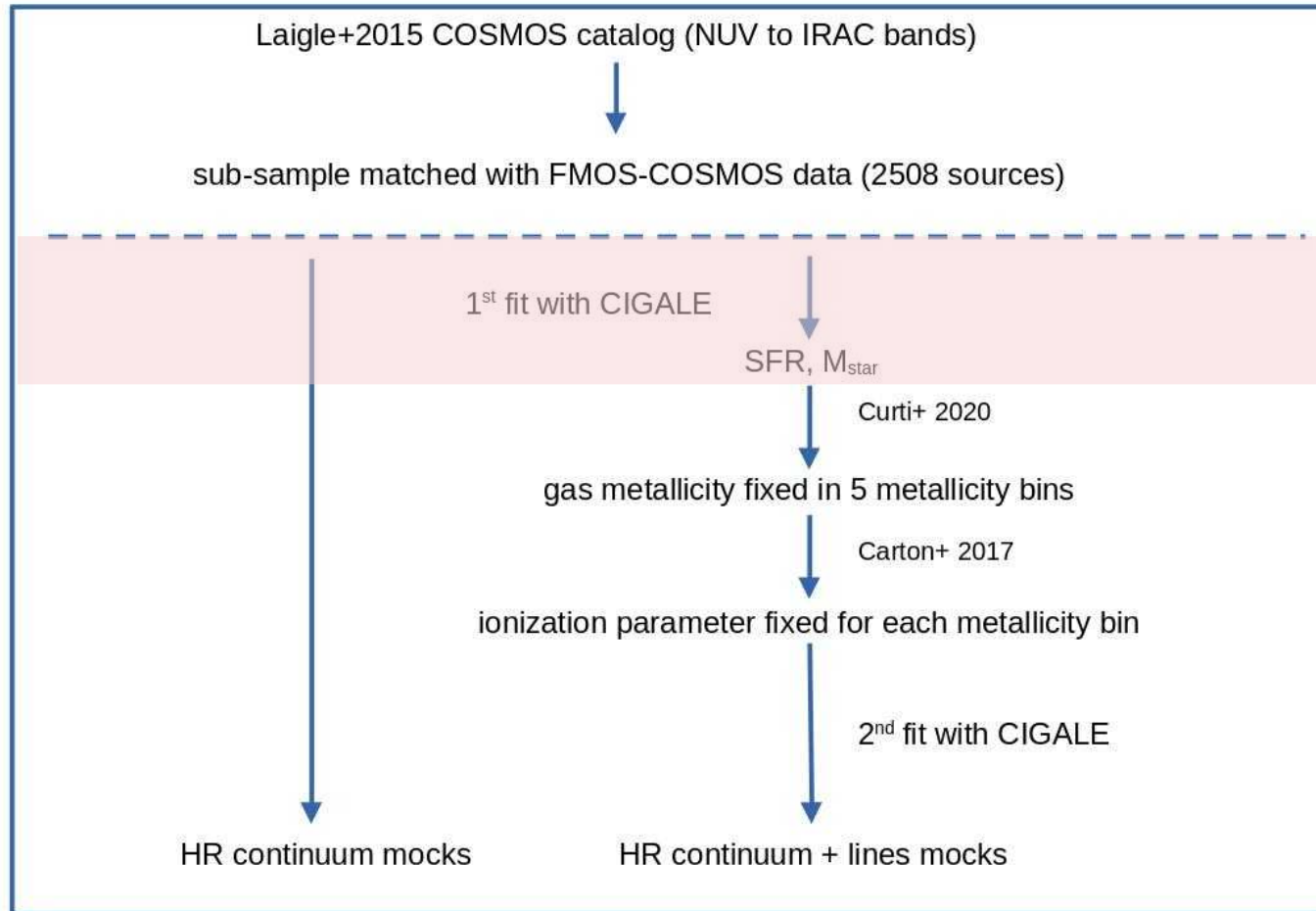
- cross-matched of COSMOS2015 (Laigle et al. 2016) with the Subaru/FMOS-COSMOS catalog (Kashino et al., 2013 and Silverman et al. 2015) to get a 2508 galaxies sample
- $0.6 < z < 1.6$ H α and [OIII]5007 in MOONS spectral range
- UV-to-MIR SED fit
- 853 detected in H α



→ generate spectral templates

Mock spectra generation procedure

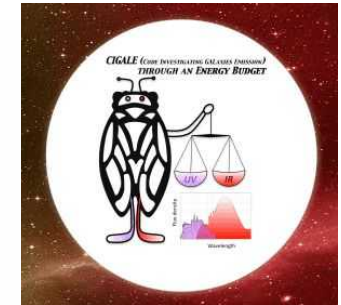
step 1



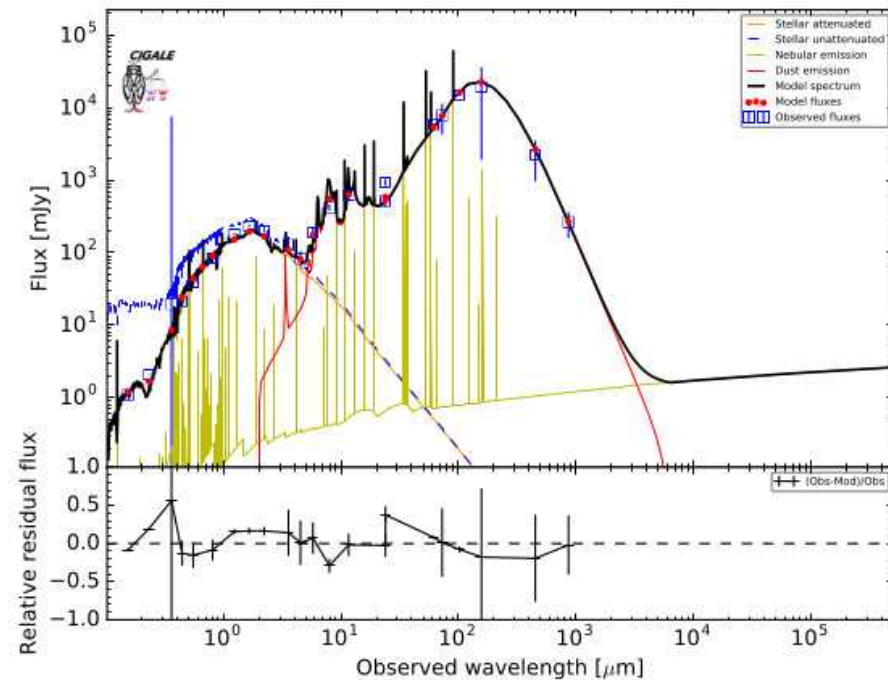
Step 1 : Fit of the UV-to-MIR photometric data

CIGALE = Code Investigating GALaxy Emission

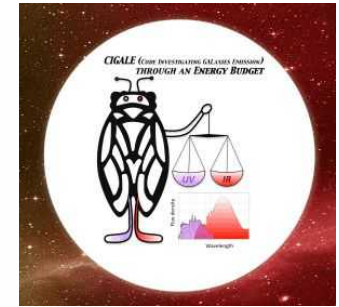
- energy balance principle
- a SED fitting code (Bayesian analysis)
- produces mock spectra to compare with observations



Best model for NGC0958 at $z = 0.019$. Reduced $\chi^2 = 1.9$

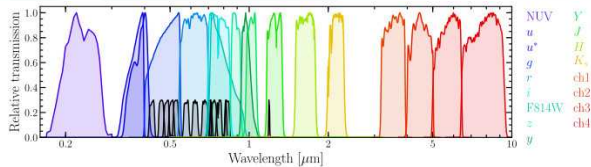


Step 1 : Fit of the UV-to-MIR photometric data



CIGALE = Code Investigating GALaxy Emission

- energy balance principle
- a SED fitting code (Bayesian analysis)
- produces mock spectra to compare with observations



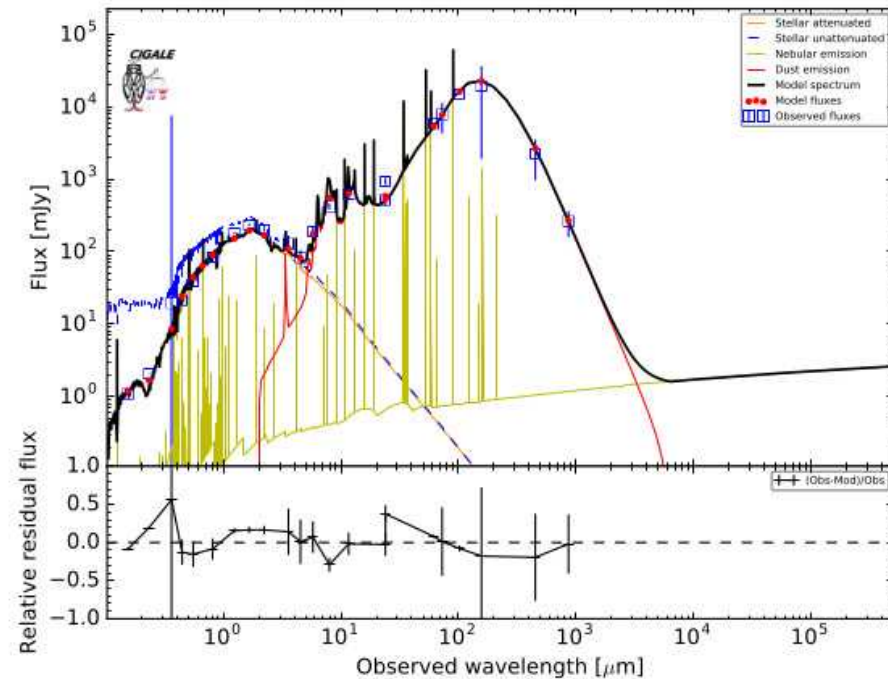
fit of the UV-to-MIR photometric data

→ SFH (star formation rates, stellar mass)

SFH = delayed + burst

Calzetti attenuation curves for the lines and for the continuum

Best model for NGC0958 at z = 0.019. Reduced $\chi^2=1.9$

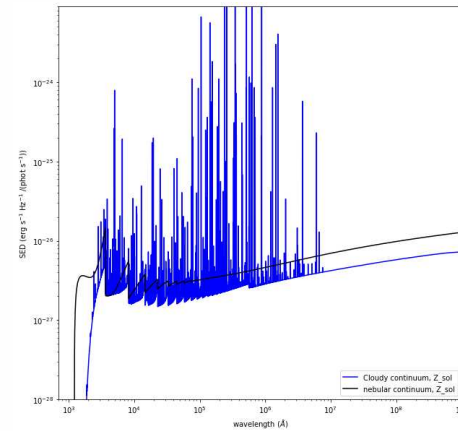
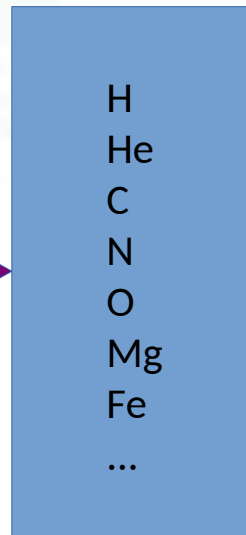


Nebular emission lines modeling

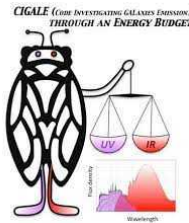
density n_H
metallicity Z_O
elementary atomic abundances

the CIGALE nebular emission module

ionizing radiation field :
shape + intensity



nebular continuum + emission lines



(U, n_H, Z_O)

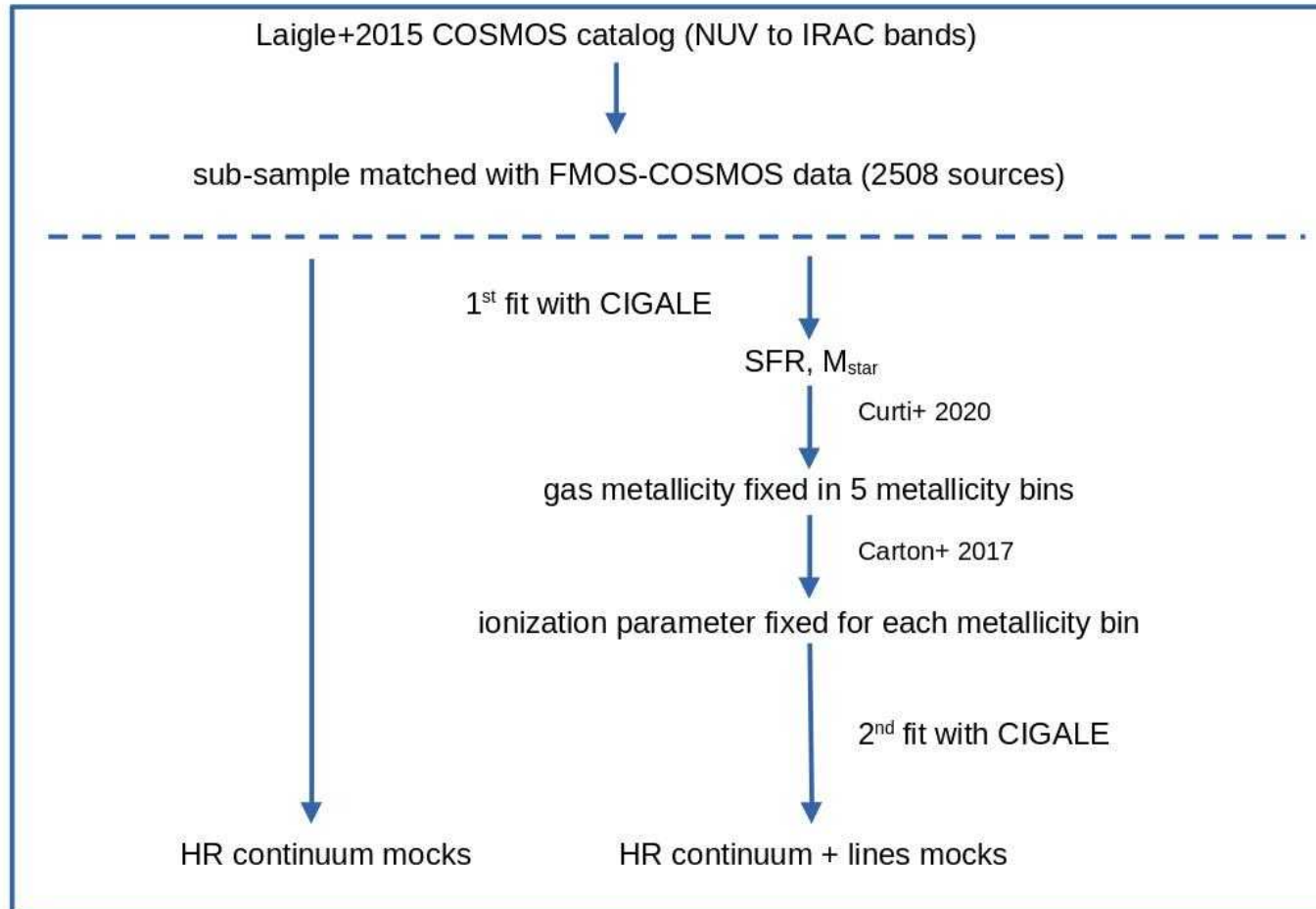
Cloudy & Associates

Photoionization simulations for the discriminating astrophysicist since 1978

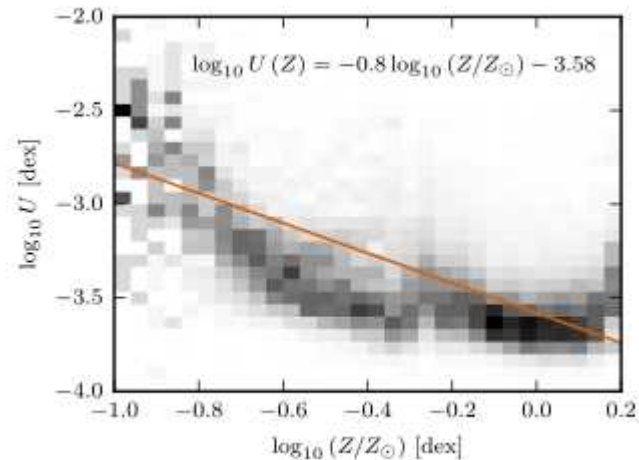
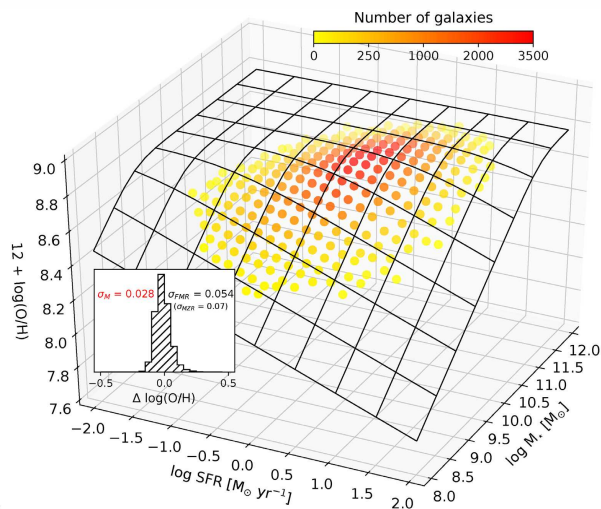
fixed extinction MW + Calzetti $E_{B-V} = 0.44$
variable extinction on line flux fitting

1. calculate the abundances of each species (chemical reaction networks)
2. calculate the populations for each level for each species (collisional/radiative level excitation)
3. compute radiative transfer for each emission line
4. generate a library of emission lines templates as a function of a set of parameters (U, n_H, Z_O)

Mock spectra generation procedure



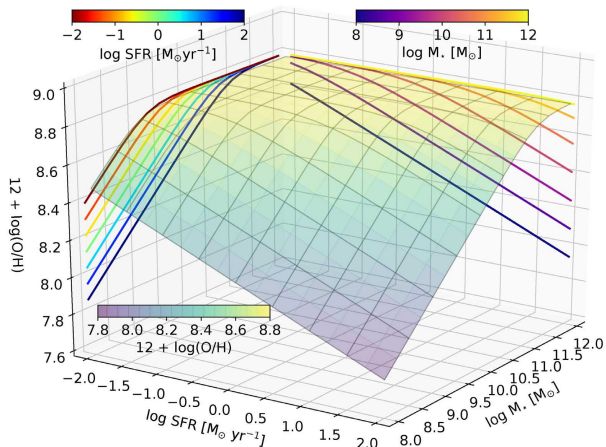
Nebular emission lines modeling



metallicity – ionization parameter relation

$$\log_{10} U (Z) = -0.8 \log_{10} Z/Z_{\odot} - 3.58$$

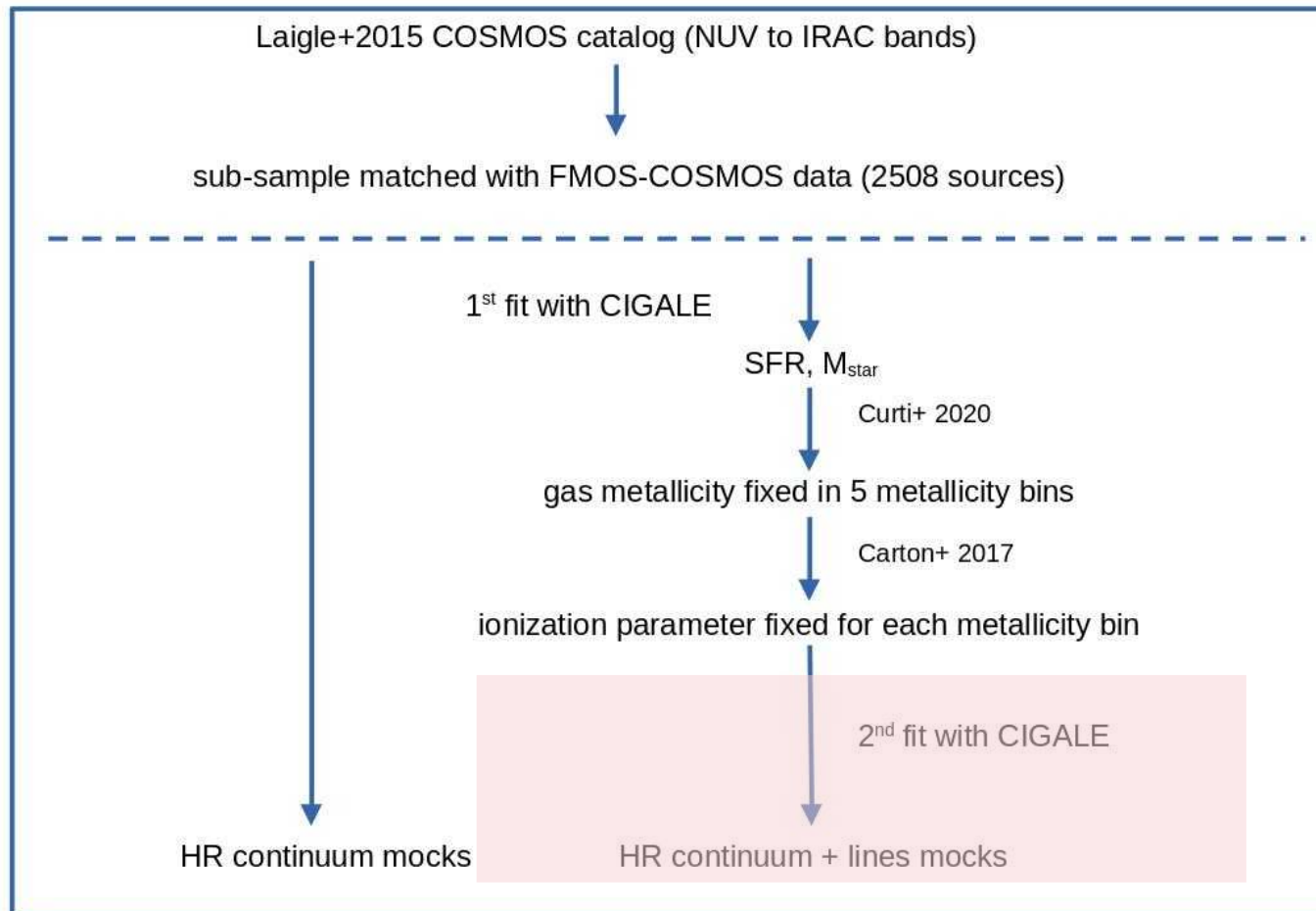
Carton et al. MNRAS 2017



mass-metallicity -SFR relation
Curti et al. 2020

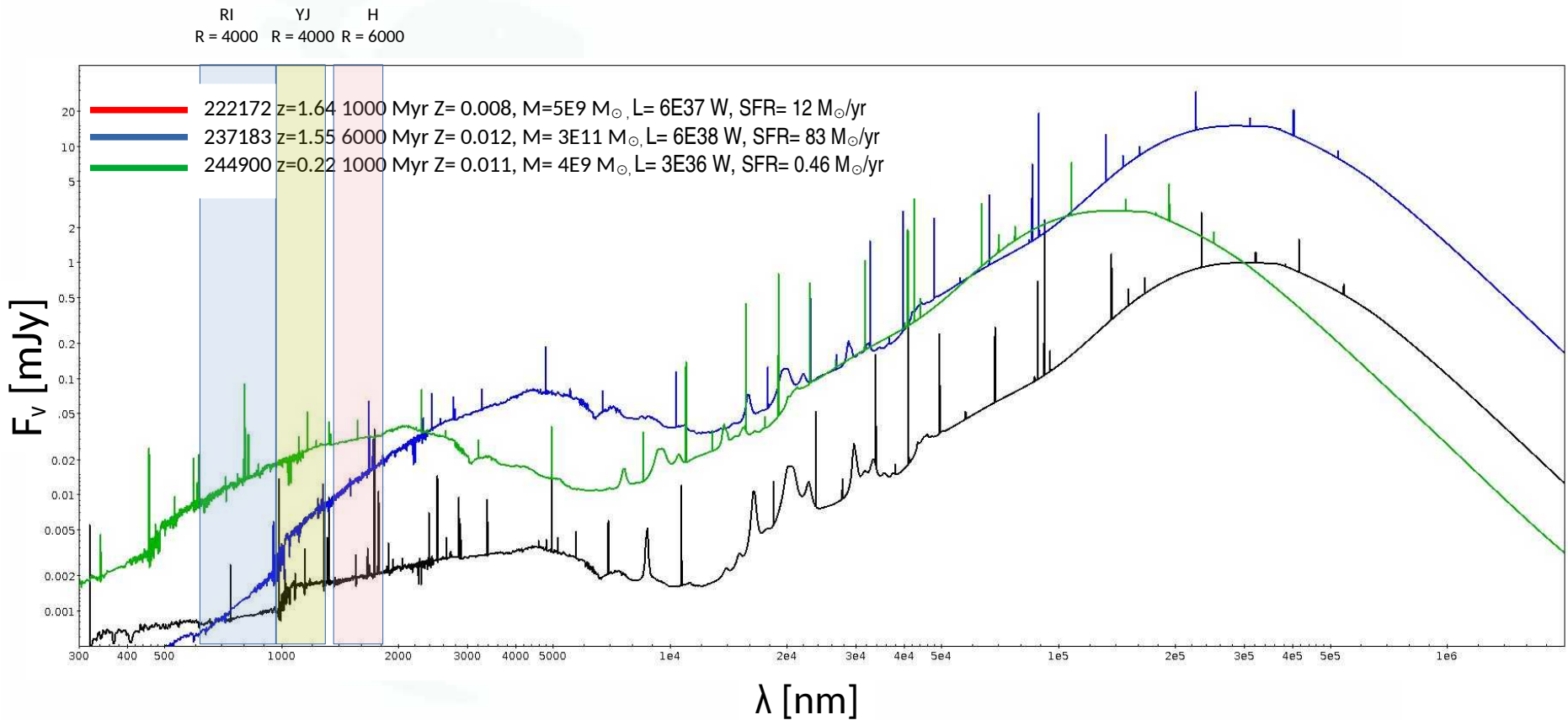
gas metallicity → star metallicity

Mock spectra generation procedure



step 2

Step 2 : mock catalog on the COSMOS field

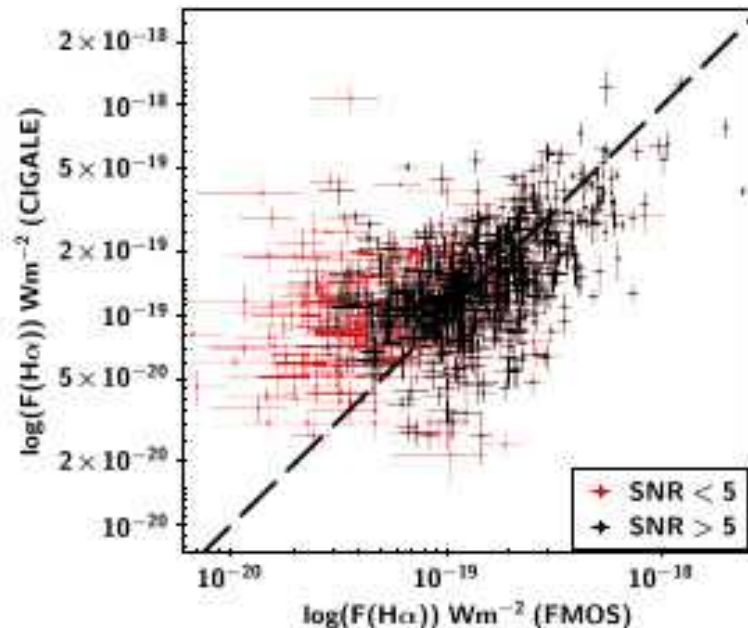


mock spectra for 2508 galaxies

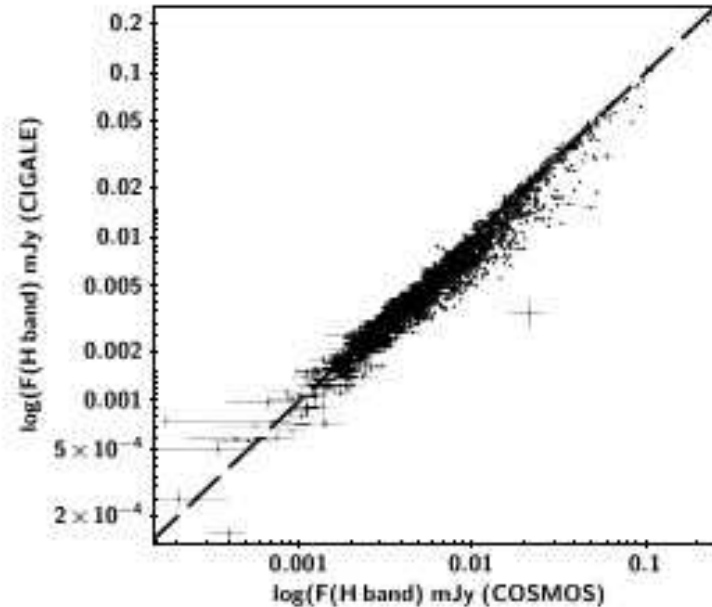
- continuum only
- continuum + lines (U fixed)

Results: comparison of observed and modelled flux

self-consistency checks

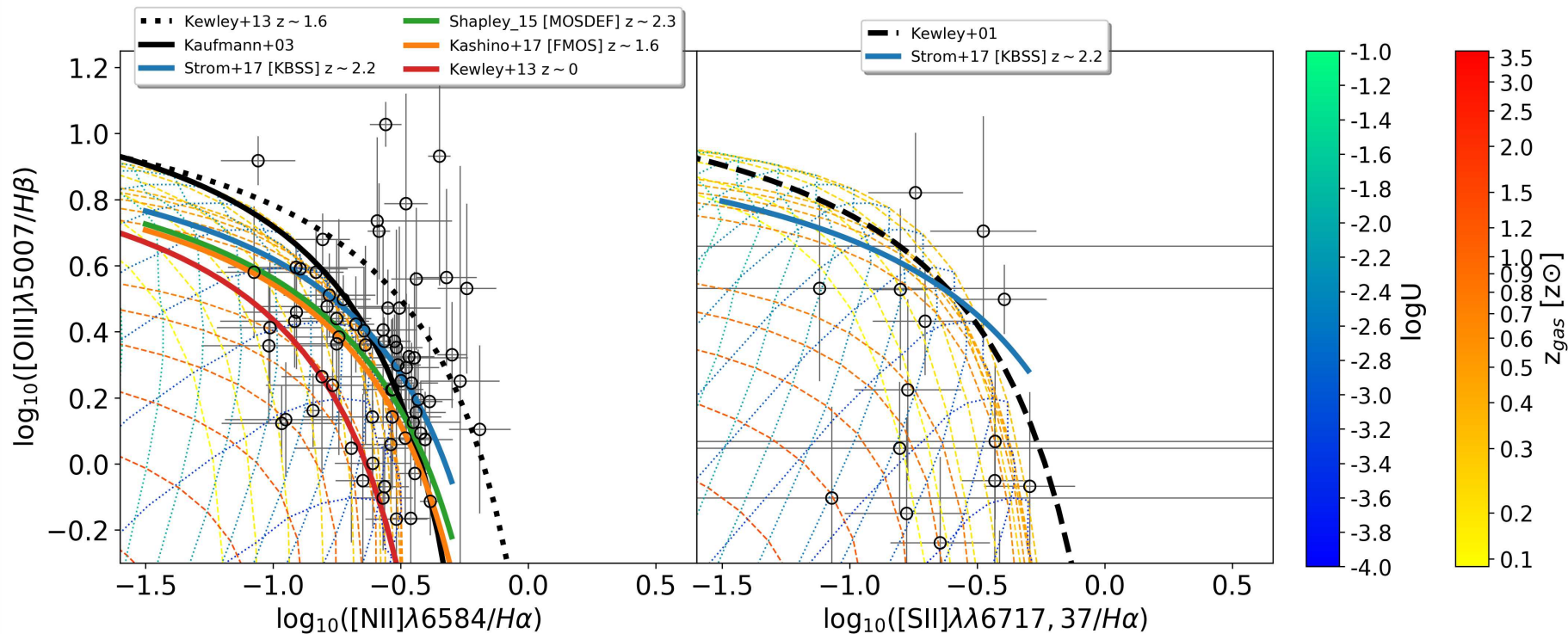


$\text{H}\alpha$ fluxes. The agreement is quite good except for 6% of the sample plotted in red, correspond to measured fluxes with an SNR lower than 5



H-band fluxes: the agreement is excellent for the whole sample

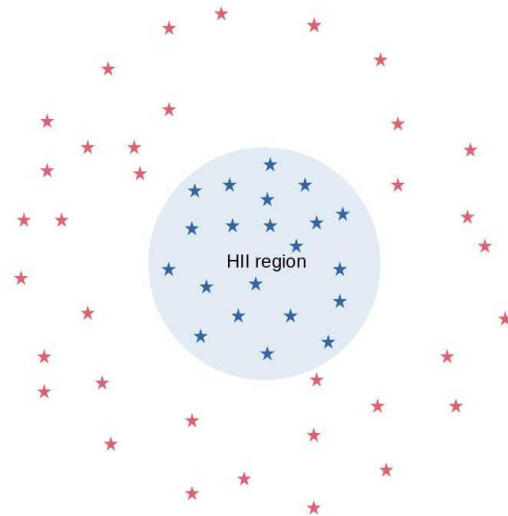
Results: excitation diagnostic diagrams



Baldwin-Phillips-Terlevich (BPT) diagrams

from Villa-Vélez et al. A&A 2021

I. Starburst regions



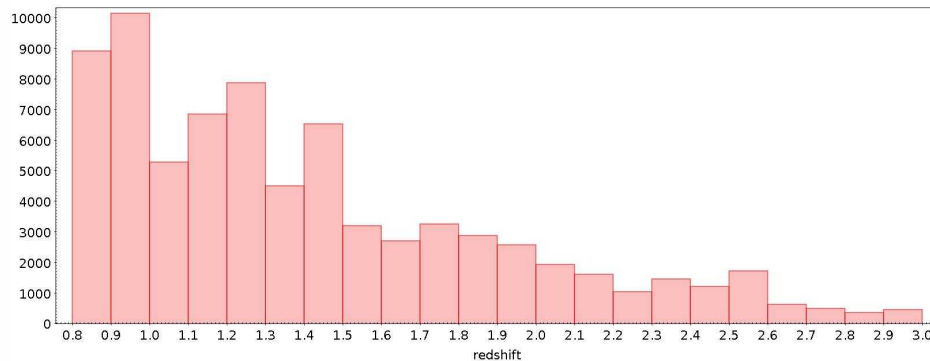
1. Technique validation on a reduced sample with spectroscopic data
2. Extension to a larger sample
3. Updates on CIGALE line fitting capacities improvements

Mock spectra on a 61872 galaxy sample from COSMOS

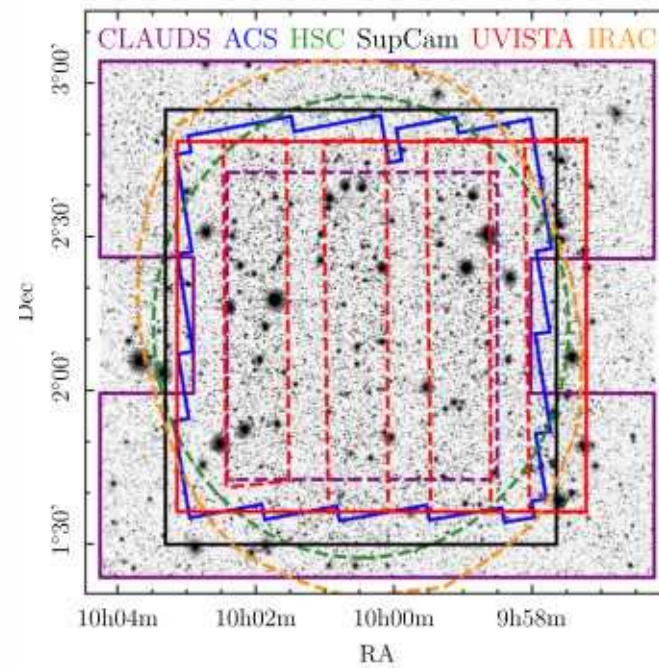
sample selection :

- the flux on the H band : $\text{mag}(H) < 23.5$ or $\text{flux} > 1.4454 \mu\text{Jy}$
- the redshift : $0.8 < z < 3$
- object inside the UltraVista stripes deep region (1.792 deg^2 , Moneti et al. 2019)
- good HSC imaging quality (2.75 deg^2)
- good Subprime-Cam imaging quality (1.918 deg^2)
- reduced $\chi^2 < 5$ criterion

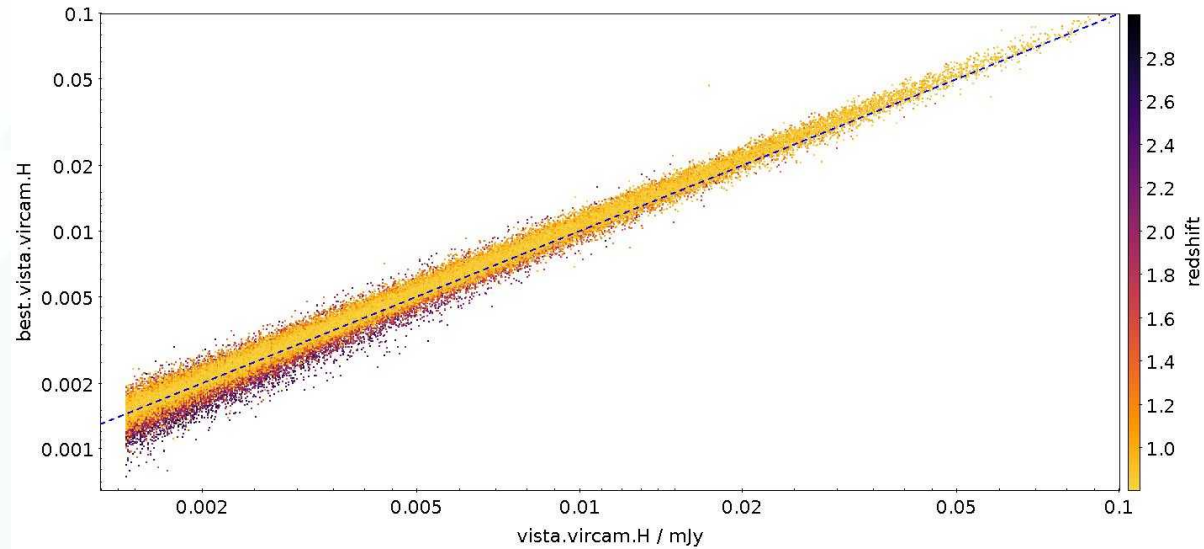
→ 1.792 deg^2 area, 61872 galaxies



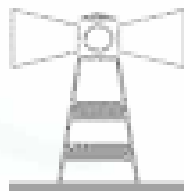
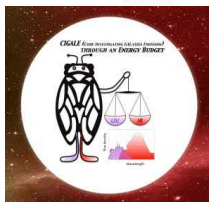
Weaver et al. ApJS 2022



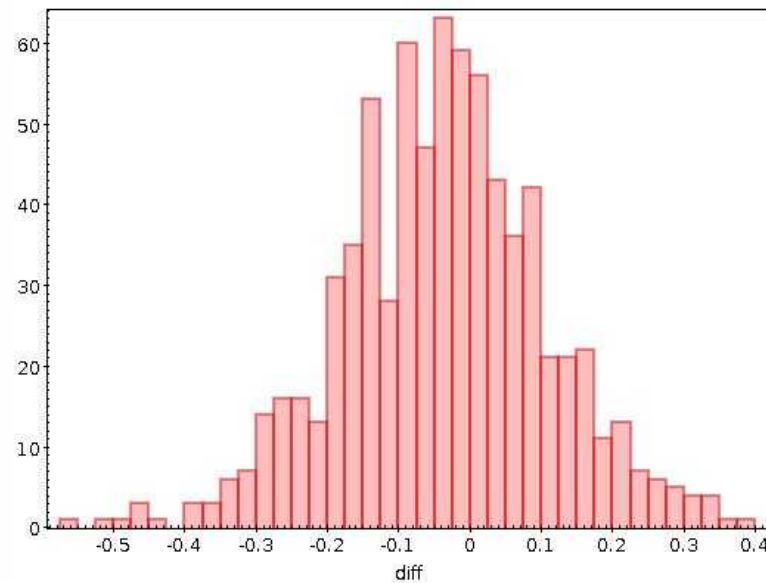
Consistency checks



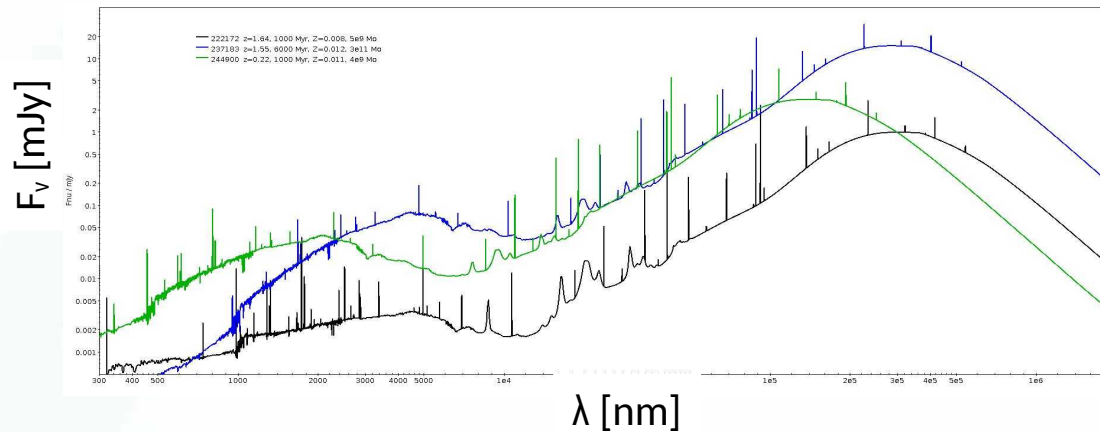
difference in M_{star}
CIGALE vs Le Phare



Weaver et al. ApJS 2022



Results: a library of spectral templates from COSMOS

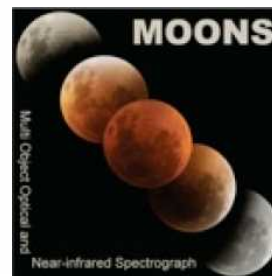


- freely available on the GASP/ASPIX LAM database

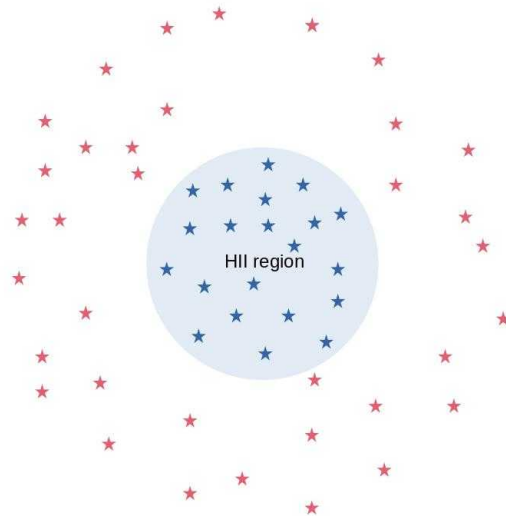


Galaxy redshifts and physical parameters

- processed through the VLT/MOONS ETC



I. Starburst regions



1.1. Technique validation on a reduced sample with spectroscopic data

1.2. Extension to a larger sample

1.3. Updates on CIGALE line fitting capacities improvements



Updates on CIGALE line fitting capacities improvements

on HII regions

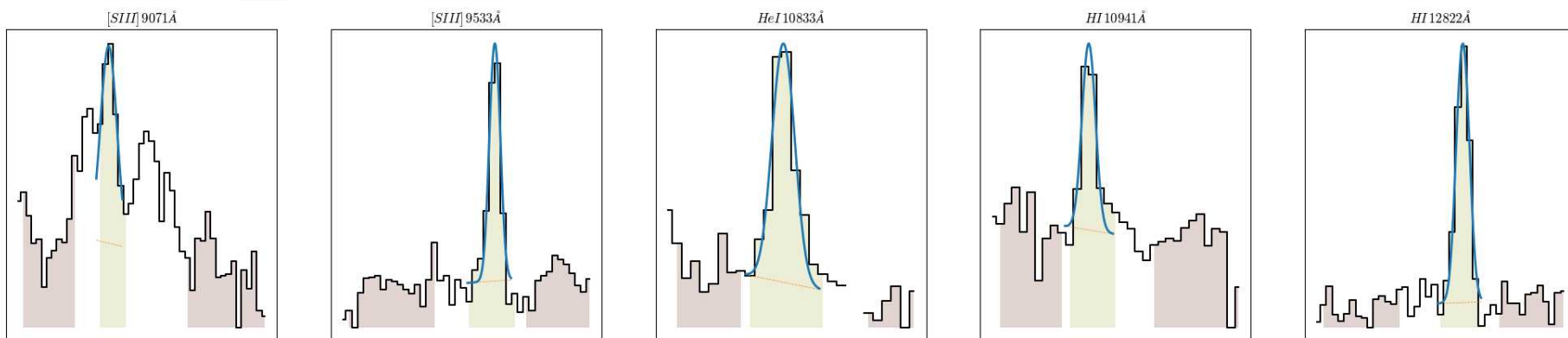
Use of the BPASS SSP library

SED fitting with equivalent width modeling in CIGALE

CIGALE computes the EWs from the modeled SED :

- linear fit of the continuum taken on each side of the line (orange)
- emission line with disentangled EWs for blended lines (green)

JWST observations with NIRCam and NIRSpec gratings, CEERS survey

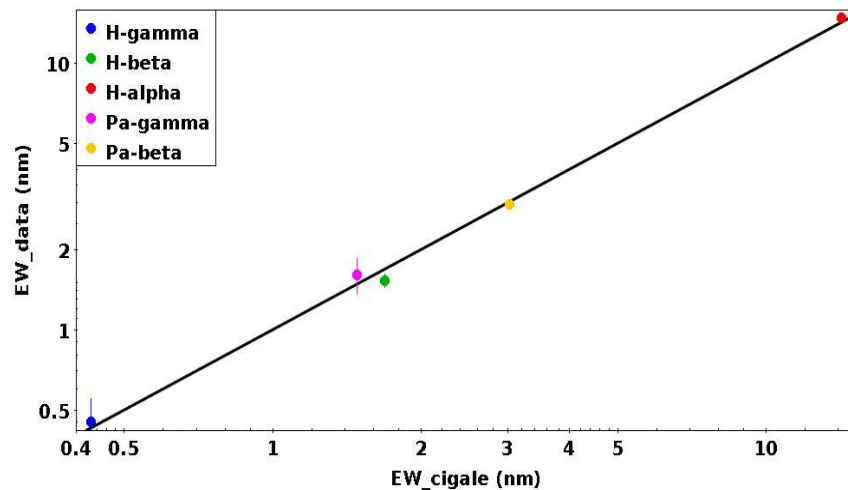
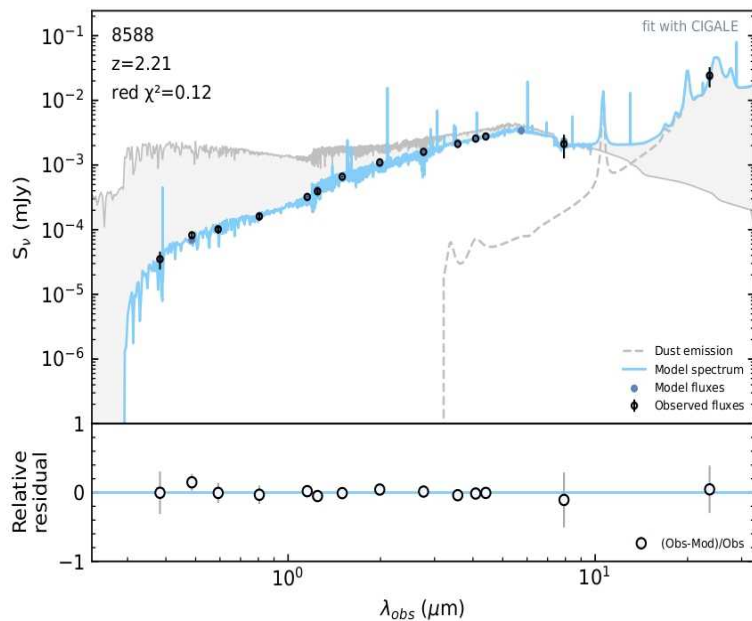


Credit : V. Fernandez



Updates on CIGALE line fitting capacities improvements

on HII regions

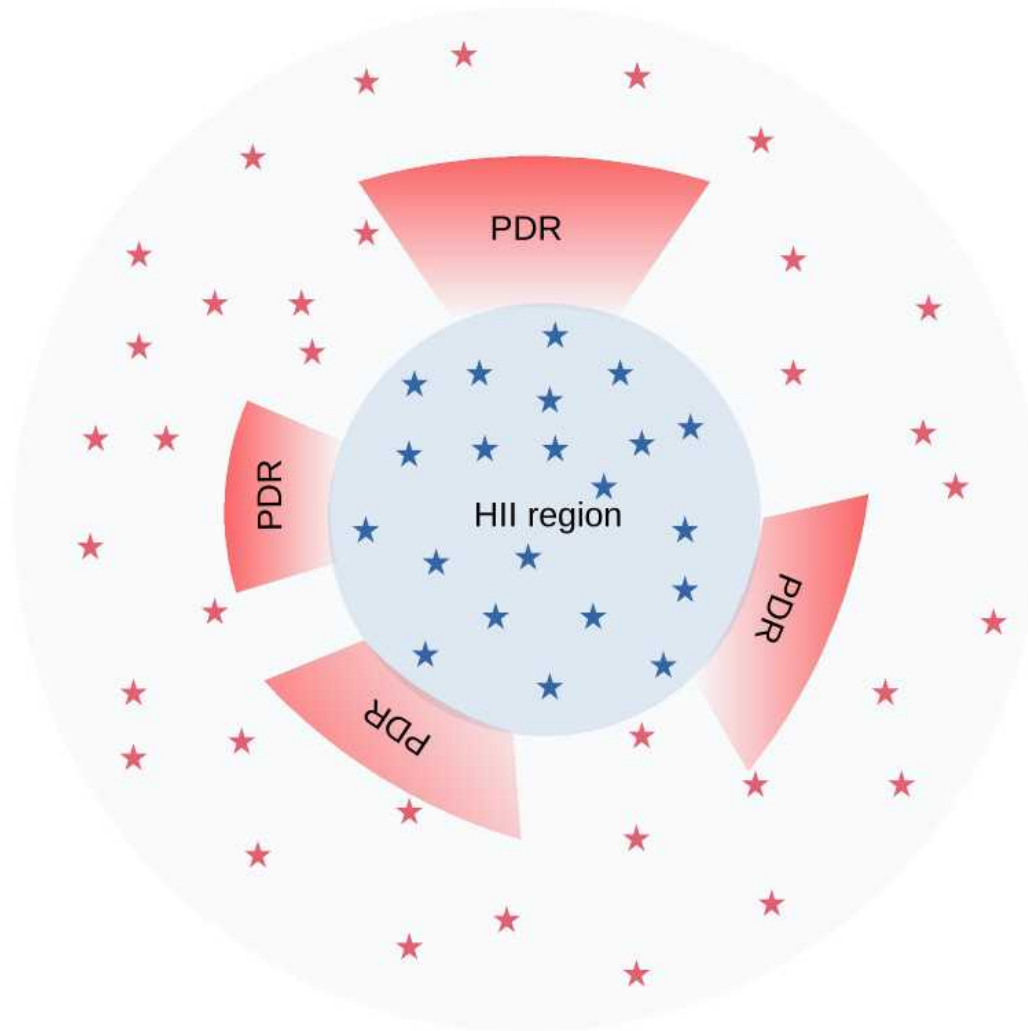


good agreement between the fit and the data

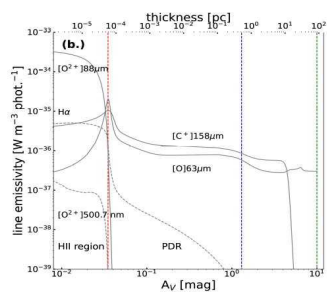
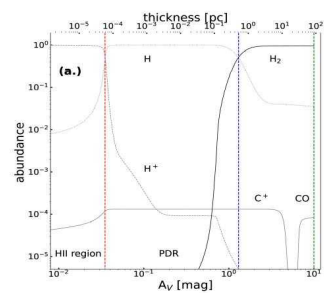
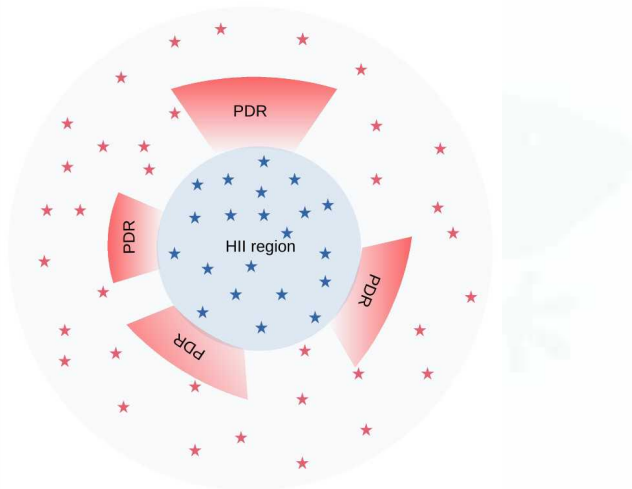
Fit combining CFHT, HST, NIRCcam, IRAC and Spitzer photometry with 5 emission lines EWs from NIRSpc

→ new EW CIGALE module adapted for MOONS

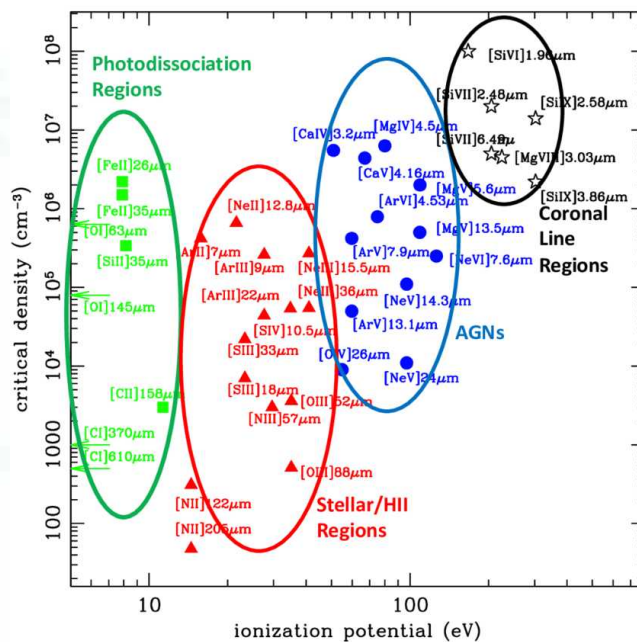
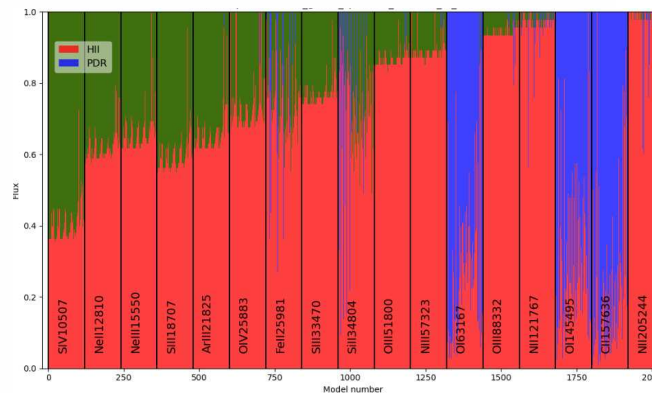
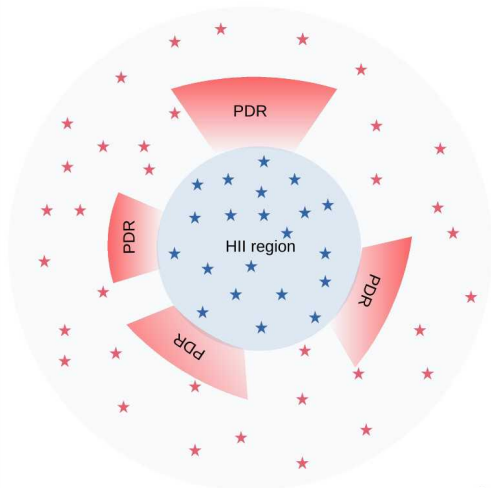
II. Starburst regions and photon dominated regions



Structure of a Photon Dominated Region (PDR)

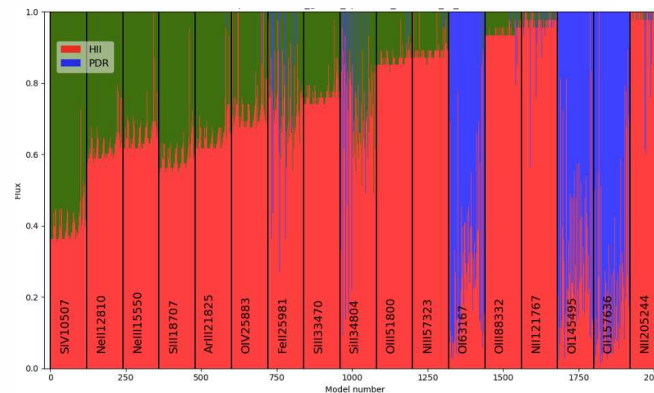
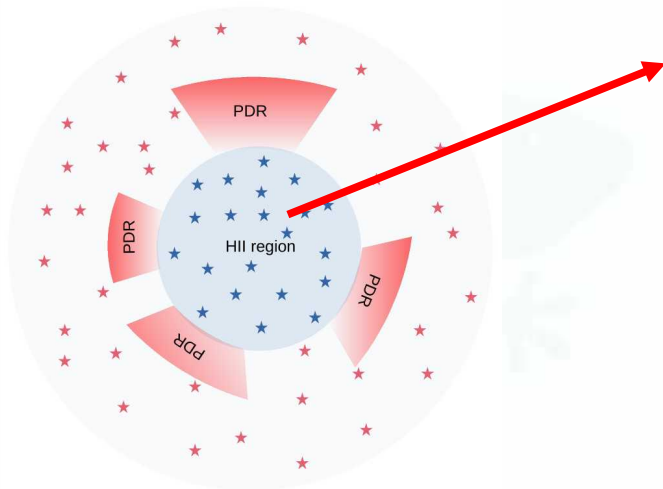


Structure of a Photon Dominated Region (PDR)



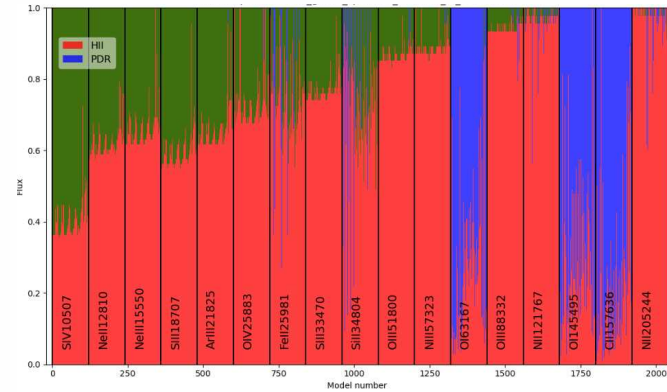
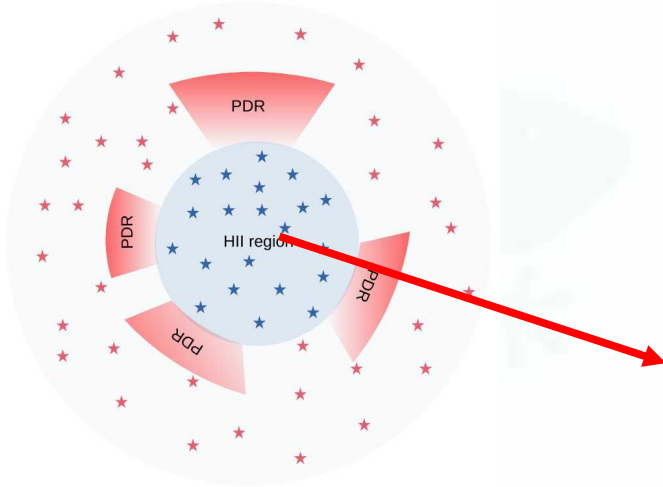
Spinoglio et al. PASA 2017

Structure of a Photon Dominated Region (PDR)



$$I = (1 - f_{\text{cov}}) \times I_{\text{HII}} \times g_{\text{att}}(\lambda)$$

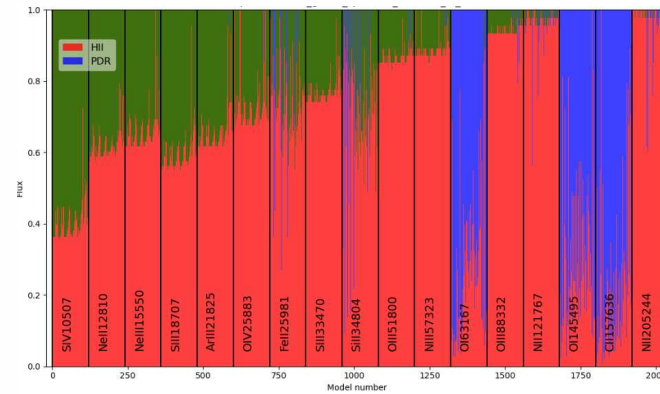
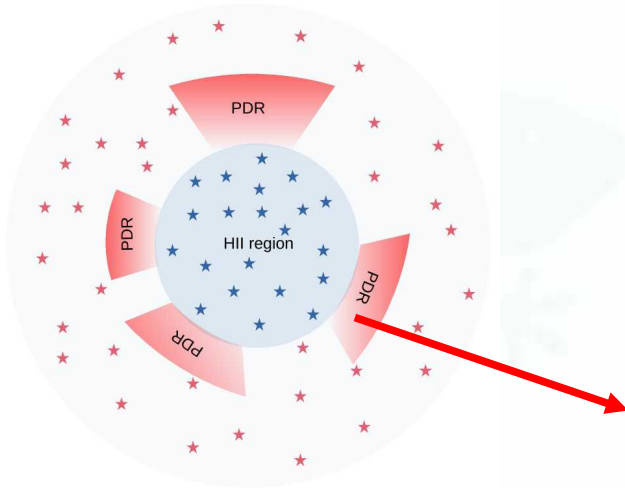
Structure of a Photon Dominated Region (PDR)



I =

$$f_{\text{cov}} \times (I_{\text{HII}} * 10^{-A(\lambda)} + I_{\text{PDR}})$$

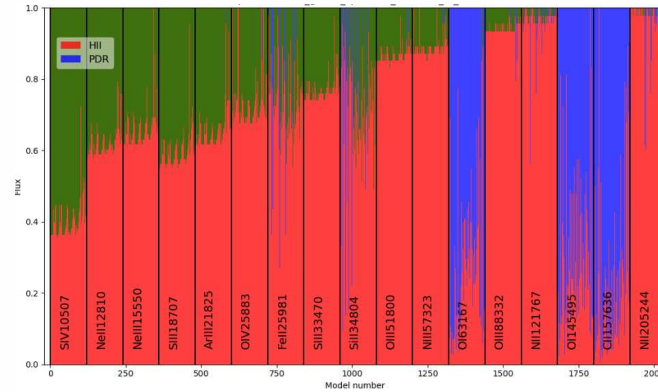
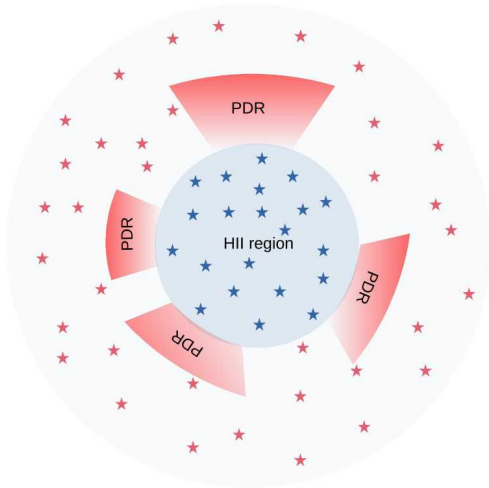
Structure of a Photon Dominated Region (PDR)



I =

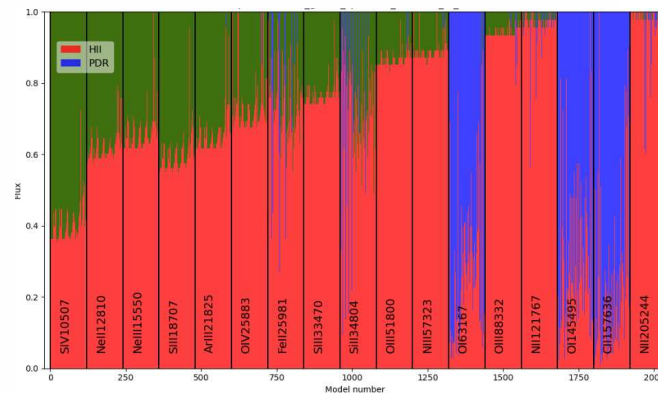
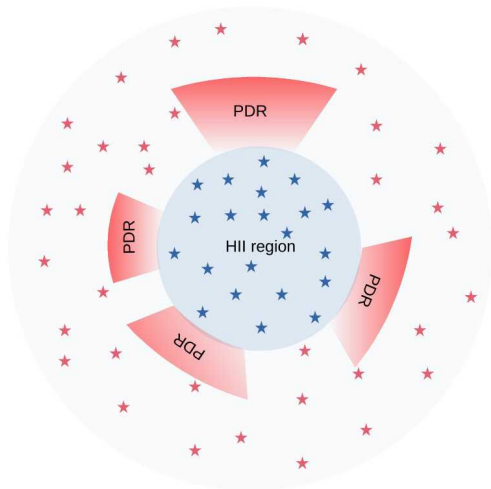
$$f_{\text{cov}} \times (I_{\text{HII}} * 10^{-A(\lambda)} + I_{\text{PDR}})$$

Structure of a Photon Dominated Region (PDR)



$$I = (1 - f_{\text{cov}}) \times I_{\text{HII}} \times g_{\text{att}}(\lambda) + f_{\text{cov}} \times (I_{\text{HII}} * 10^{-A(\lambda)} + I_{\text{PDR}})$$

Structure of a Photon Dominated Region (PDR)



$$I = (1 - f_{\text{cov}}) \times I_{\text{HII}} \times g_{\text{att}}(\lambda) + f_{\text{cov}} \times (I_{\text{HII}} * 10^{-A(\lambda)} + I_{\text{PDR}})$$

↑
no dust

↑
no dust

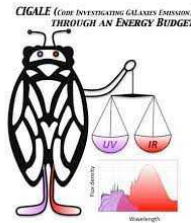
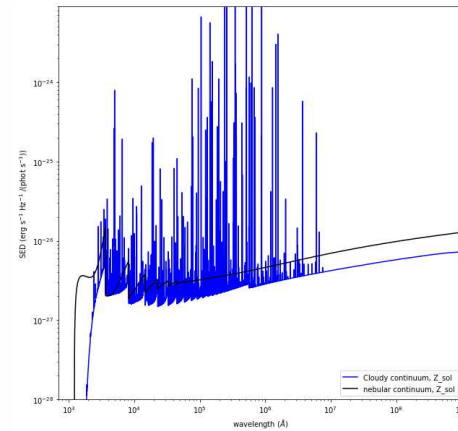
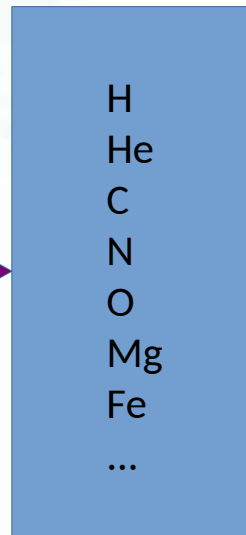
↑
dust

Nebular emission lines modeling

density n_H
metallicity Z_O
elementary atomic abundances

the CIGALE nebular emission module

ionizing radiation field :
shape + intensity



(U, n_H, Z_O)

nebular continuum + emission lines

Cloudy & Associates

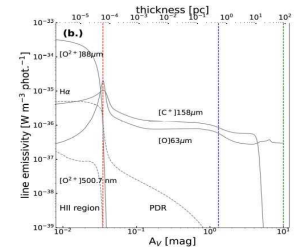
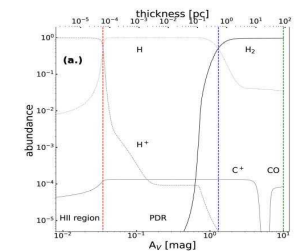
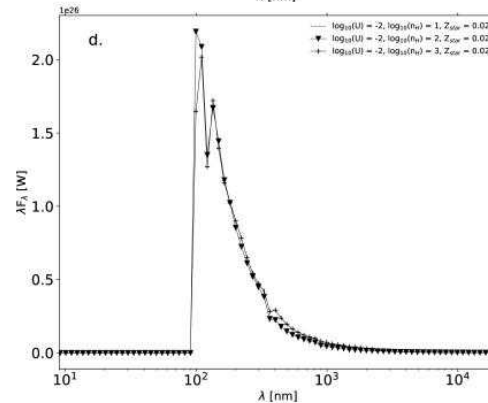
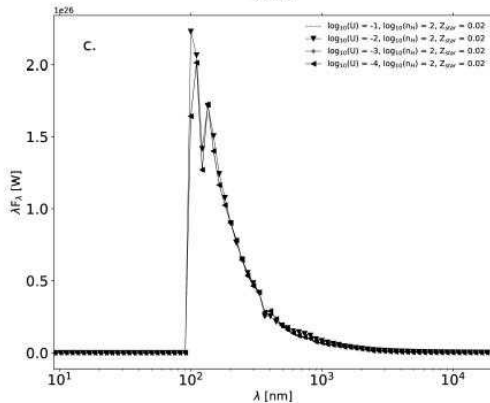
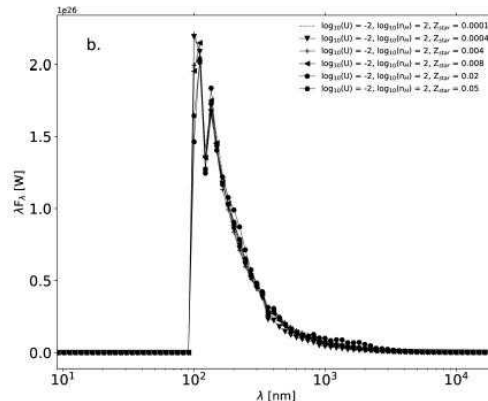
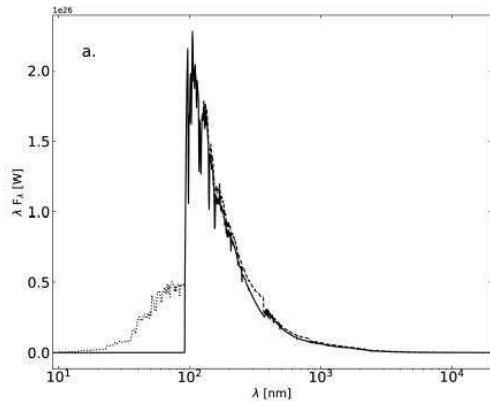
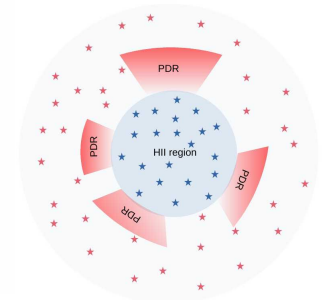
Photoionization simulations for the discriminating astrophysicist since 1978

fixed extinction MW + Calzetti $E_{B-V} = 0.44$
variable extinction on line flux fitting

1. calculate the abundances of each species (chemical reaction networks)
2. calculate the populations for each level for each species (collisional/radiative level excitation)
3. compute radiative transfer for each emission line
4. generate a library of emission lines templates as a function of a set of parameters (U, n_H, Z_O)

The photoionizing radiation field

BC03 single stellar population (age, stellar metallicity Z_{star})
+ Chabrier ($100 M_{\odot}$) initial mass function



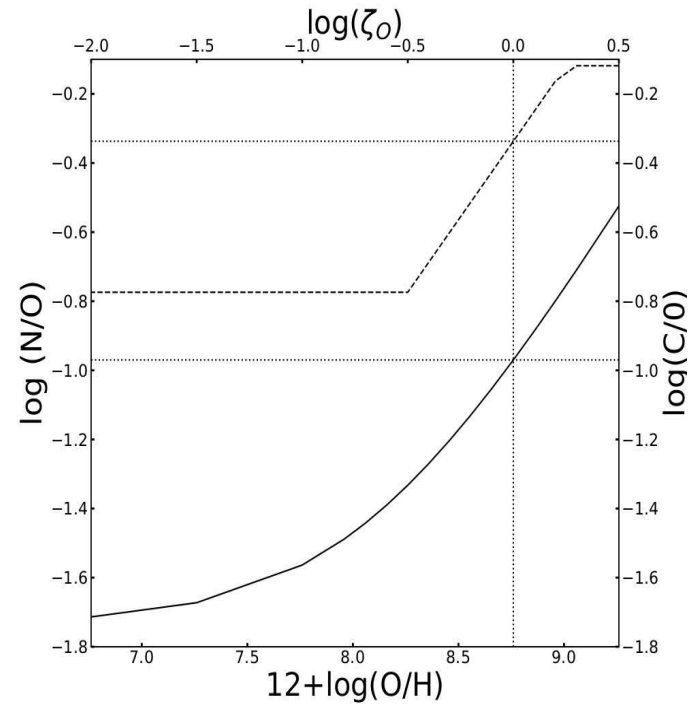
$$U \equiv \frac{Q(\text{H})}{4 \pi r_0^2 n(\text{H}) c} = \frac{N_{\text{LyC}}}{n(\text{H})}$$

Elemental abundances and metallicity

local galactic concordance model (\neq solar abundances)

element	abundance	D
H	1	1.00
He	9.77×10^{-2}	1.00
C	2.65×10^{-4}	0.50
N	6.17×10^{-5}	0.89
O	5.75×10^{-4}	0.85
Ne	1.23×10^{-4}	1.00
Mg	3.63×10^{-5}	0.08
Al	2.69×10^{-6}	0.04
Si	3.16×10^{-5}	0.15
S	1.32×10^{-5}	1.00
Ar	2.51×10^{-6}	1.00
Fe	3.31×10^{-5}	0.05

$$\zeta_0 = \frac{(O/H)}{(O/H)_{GC}}$$



$$(He/H) = 0.0835 * (1 + 0.17031 * \zeta_0)$$

$$(C/O) = 10^{-0.8} + 10^{\log(2.272 + \log(O/H))}$$

$$(N/O) = 10^{-1.732} + 10^{\log(2.19 + \log(O/H))}$$

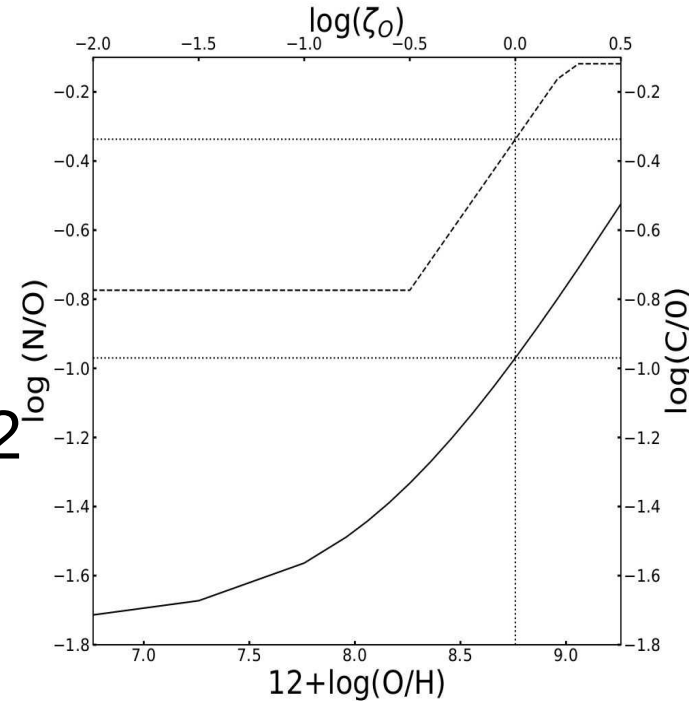
Elemental abundances and metallicity

local galactic concordance model (\neq solar abundances)

element	abundance	D
H	1	1.00
He	9.77×10^{-2}	1.00
C	2.65×10^{-4}	0.50
N	6.17×10^{-5}	0.89
O	5.75×10^{-4}	0.85
Ne	1.23×10^{-4}	1.00
Mg	3.63×10^{-5}	0.08
Al	2.69×10^{-6}	0.04
Si	3.16×10^{-5}	0.15
S	1.32×10^{-5}	1.00
Ar	2.51×10^{-6}	1.00
Fe	3.31×10^{-5}	0.05

$\zeta_{\text{O}} = 1$
 $\log \zeta_{\text{O}} = 0$
 $Z_{\odot} = 0.0142$

$$\zeta_{\text{O}} = \frac{(O/H)}{(O/H)_{GC}}$$



$$(He/H) = 0.0835 * (1 + 0.17031 * \zeta_{\text{O}})$$

$$(C/O) = 10^{-0.8} + 10^{\log(2.272 + \log(O/H))}$$

$\log \zeta_{\text{O}} < 0$: submetallic galaxies

$\log \zeta_{\text{O}} > 0$: over-metallic galaxies

$$(N/O) = 10^{-1.732} + 10^{\log(2.19 + \log(O/H))}$$

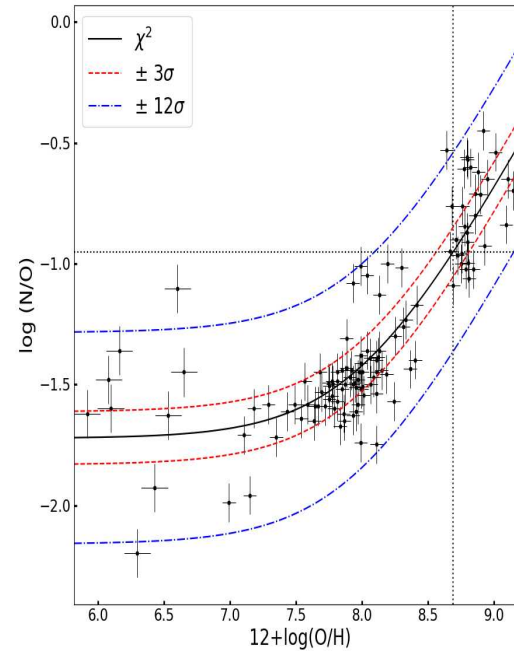
Elemental abundances and metallicity

local galactic concordance model (\neq solar abundances)

element	abundance	D
H	1	1.00
He	9.77×10^{-2}	1.00
C	2.65×10^{-4}	0.50
N	6.17×10^{-5}	0.89
O	5.75×10^{-4}	0.85
Ne	1.23×10^{-4}	1.00
Mg	3.63×10^{-5}	0.08
Al	2.69×10^{-6}	0.04
Si	3.16×10^{-5}	0.15
S	1.32×10^{-5}	1.00
Ar	2.51×10^{-6}	1.00
Fe	3.31×10^{-5}	0.05

$\zeta_{\text{O}} = 1$
 $\log \zeta_{\text{O}} = 0$
 $Z_{\odot} = 0.0142$

$$\zeta_{\text{O}} = \frac{(O/H)}{(O/H)_{GC}}$$



$$(He/H) = 0.0835 * (1 + 0.17031 * \zeta_{\text{O}})$$

$$(C/O) = 10^{-0.8} + 10^{\log(2.272 + \log(O/H))}$$

$$(N/O) = 10^{-1.732} + 10^{\log(2.19 + \log(O/H))}$$

$\log \zeta_{\text{O}} < 0$: submetallic galaxies

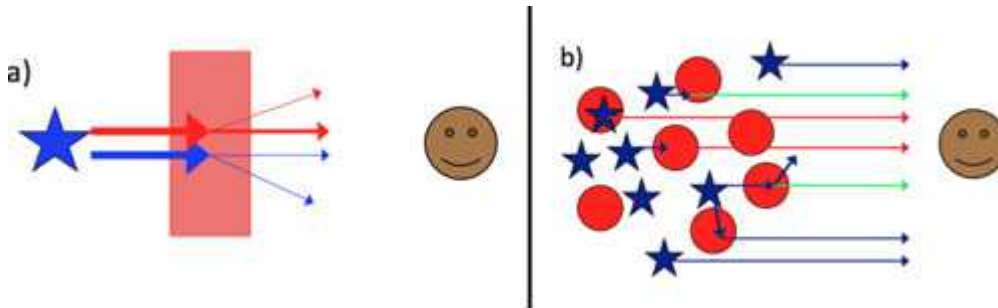
$\log \zeta_{\text{O}} > 0$: over-metallic galaxies

Dust attenuation $g_{\text{att}}(\lambda)$

$$I = (1 - f_{\text{cov}}) \times I_{\text{HII}} \times g_{\text{att}}(\lambda) + f_{\text{cov}} \times (I_{\text{HII}} * 10^{-A(\lambda)} + I_{\text{PDR}})$$

The lines are screened with the Milky Way extinction law of Cardelli et al. 1989 with $R_V = 3.1$, which is typical of diffuse media, and $A_V = 1$, which is typical of a galaxy

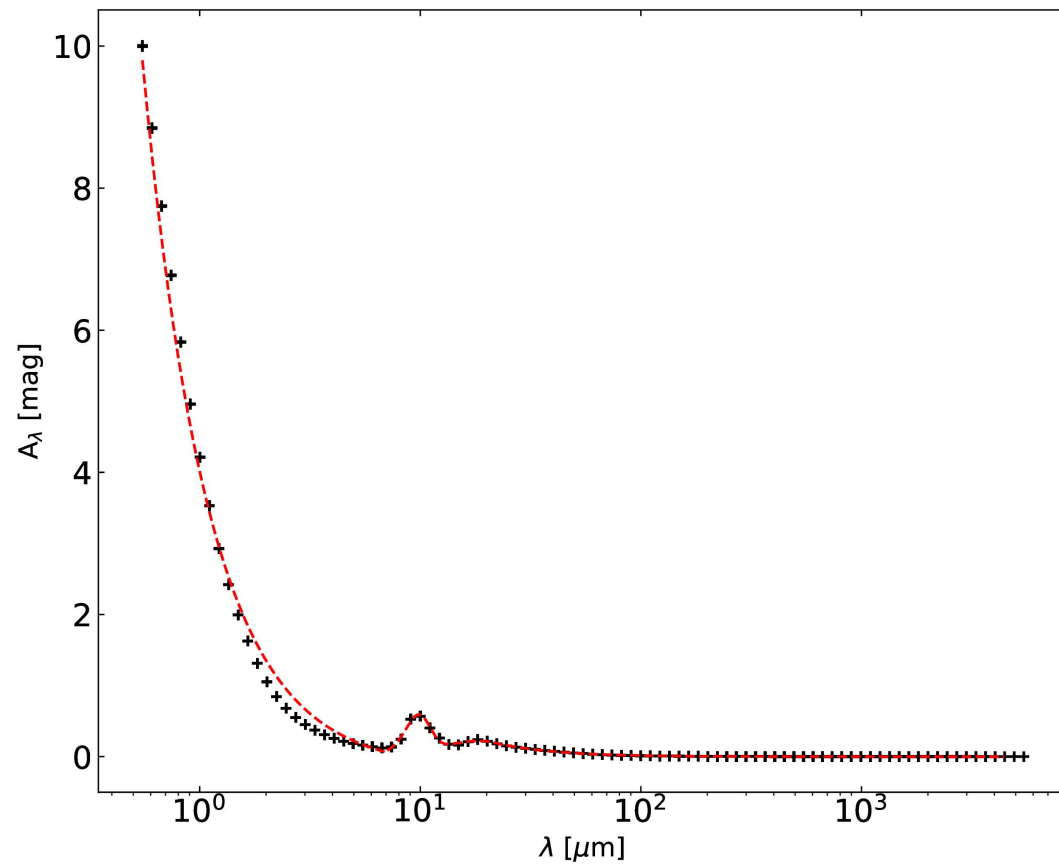
extinction \neq attenuation



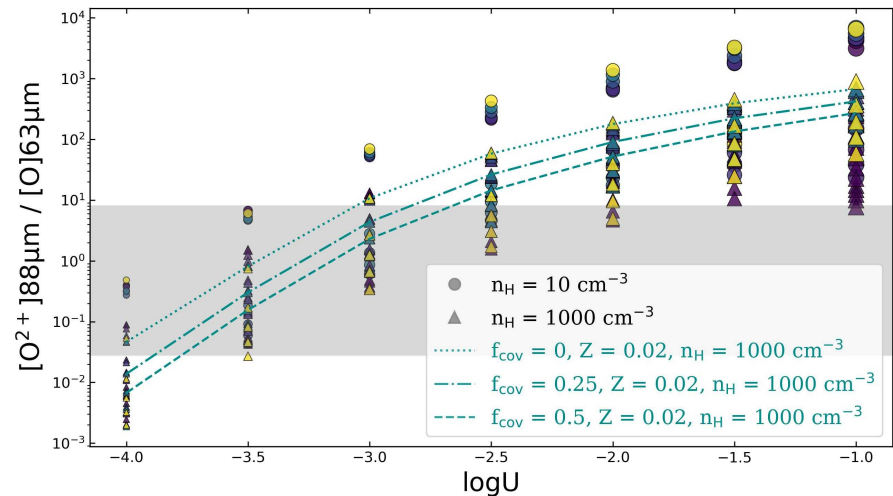
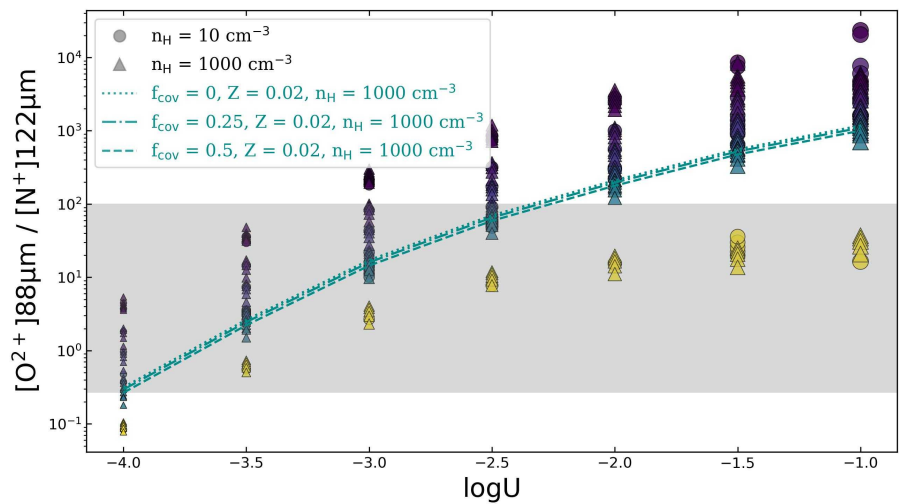
credit : D. Calzetti

Dust extinction $A(\lambda)$

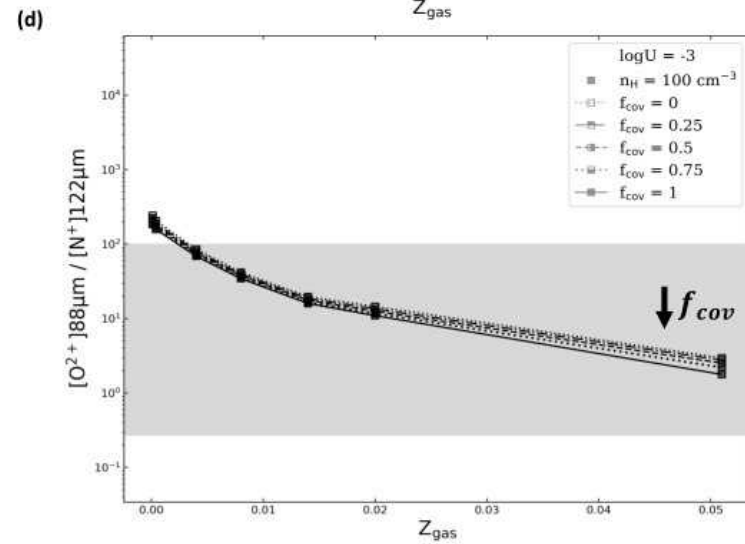
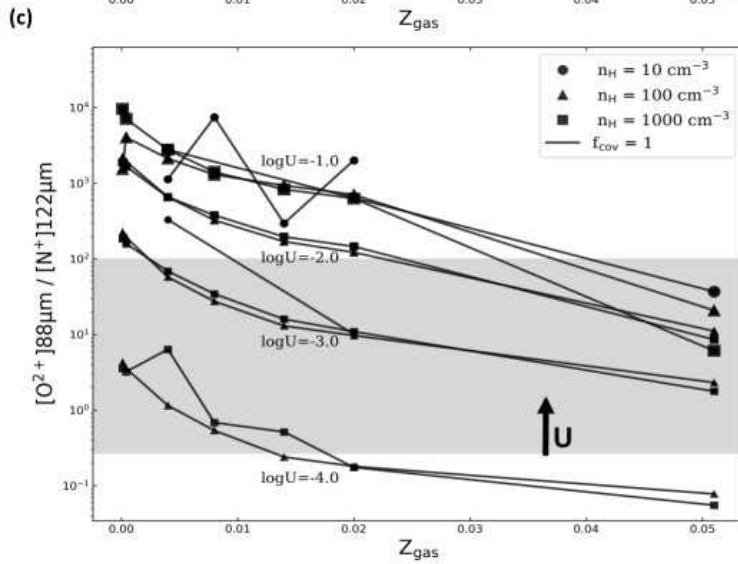
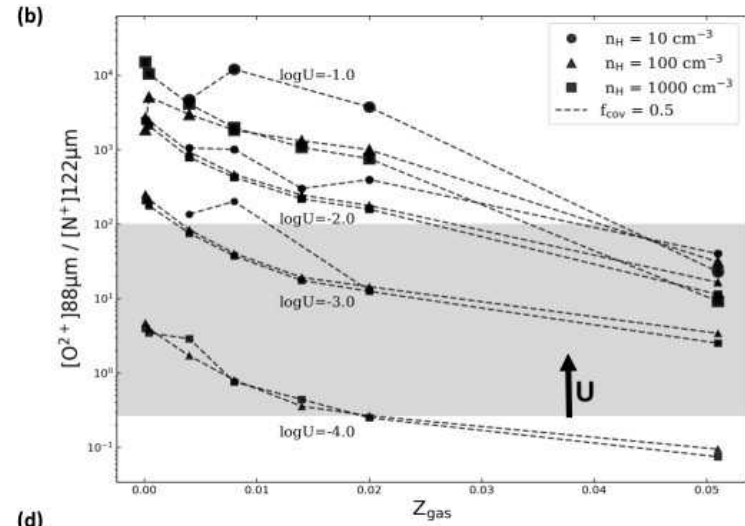
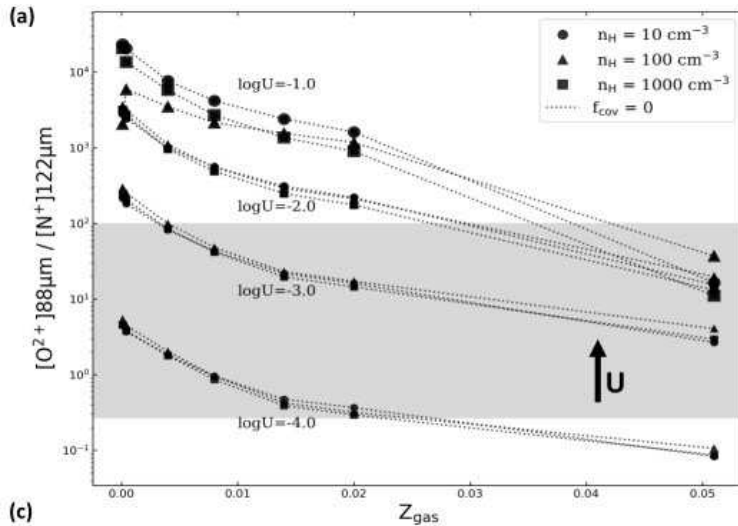
$$I = (1 - f_{\text{cov}}) \times I_{\text{HII}} \times g_{\text{att}}(\lambda) + f_{\text{cov}} \times (I_{\text{HII}} * 10^{-A(\lambda)} + I_{\text{PDR}})$$



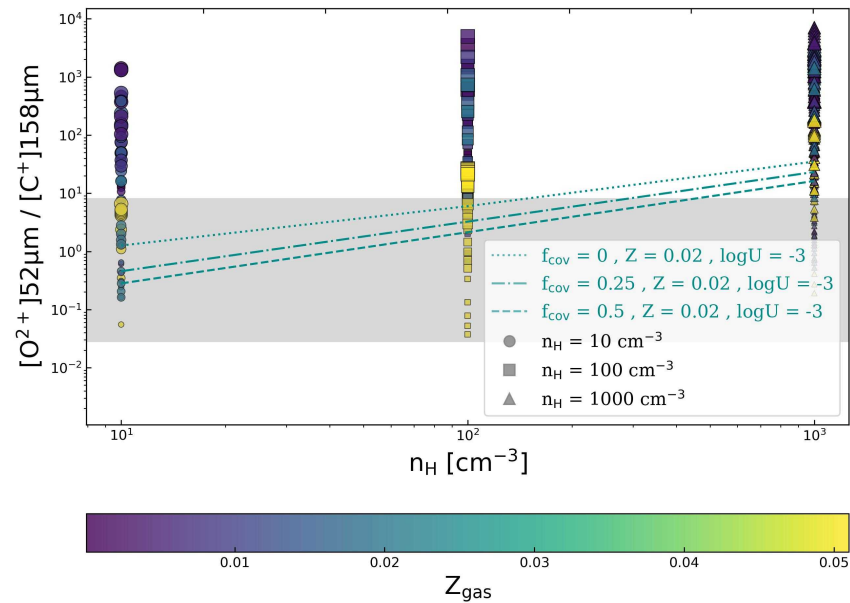
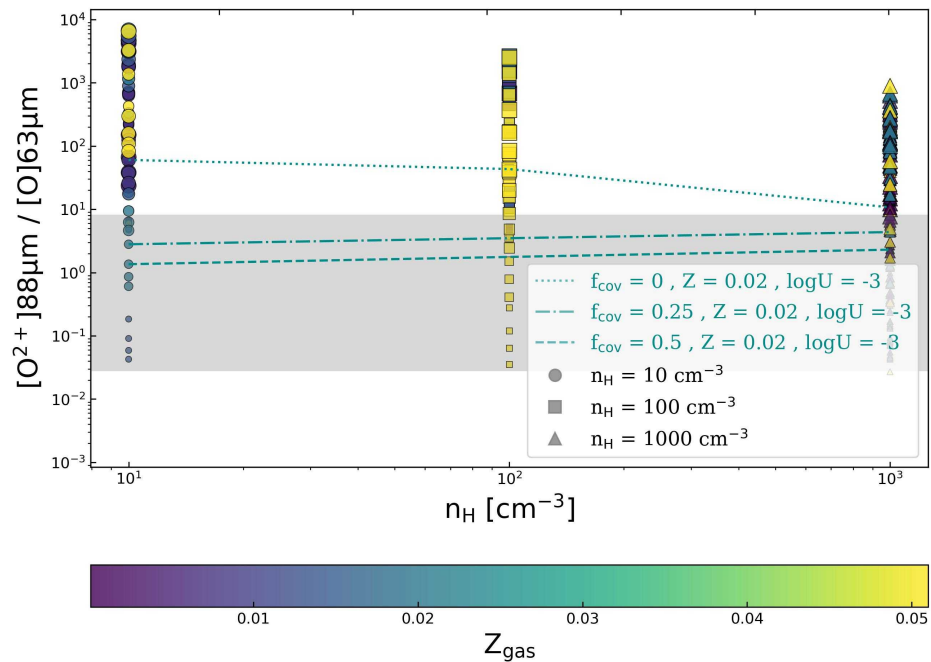
Tracers of the ionization parameters U



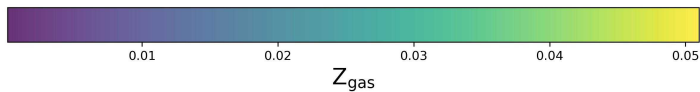
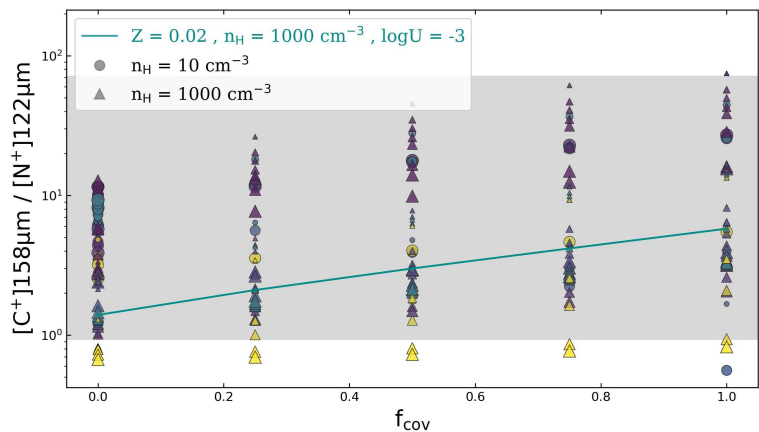
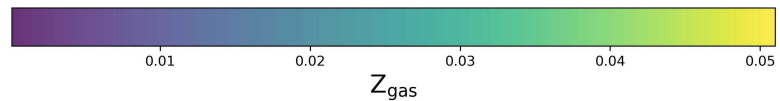
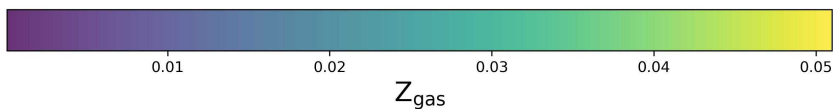
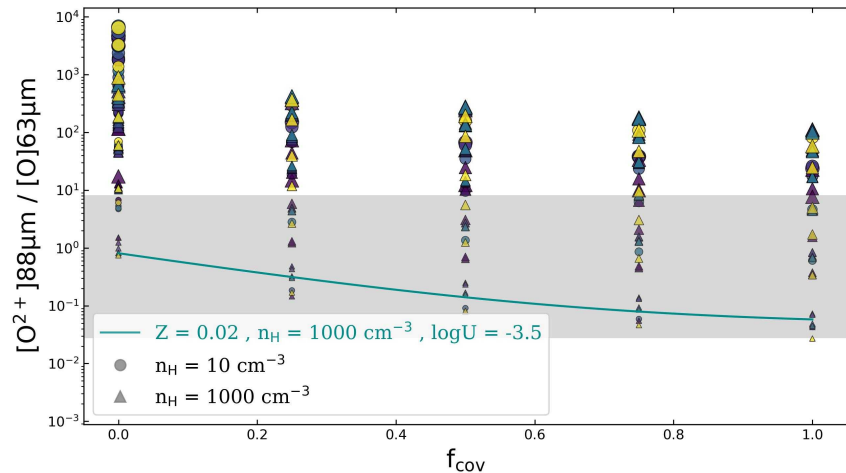
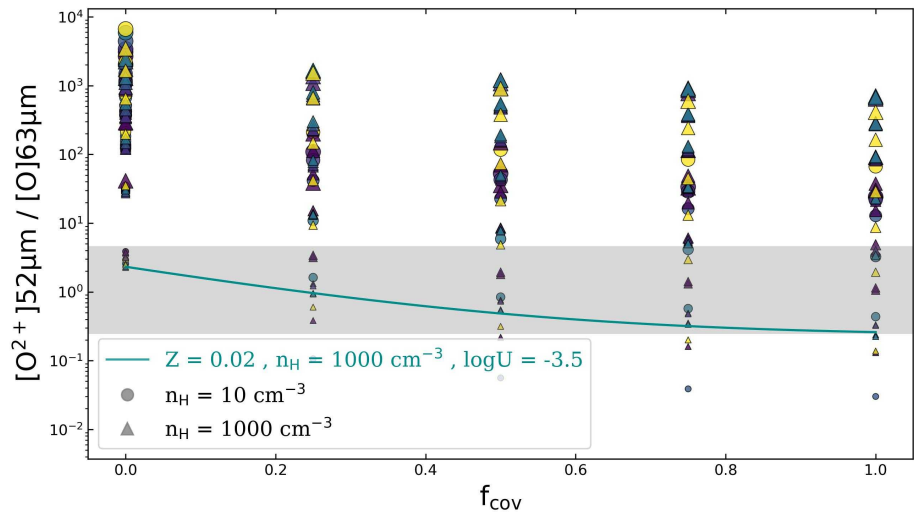
Tracers of the gas metallicity Z_{gas}



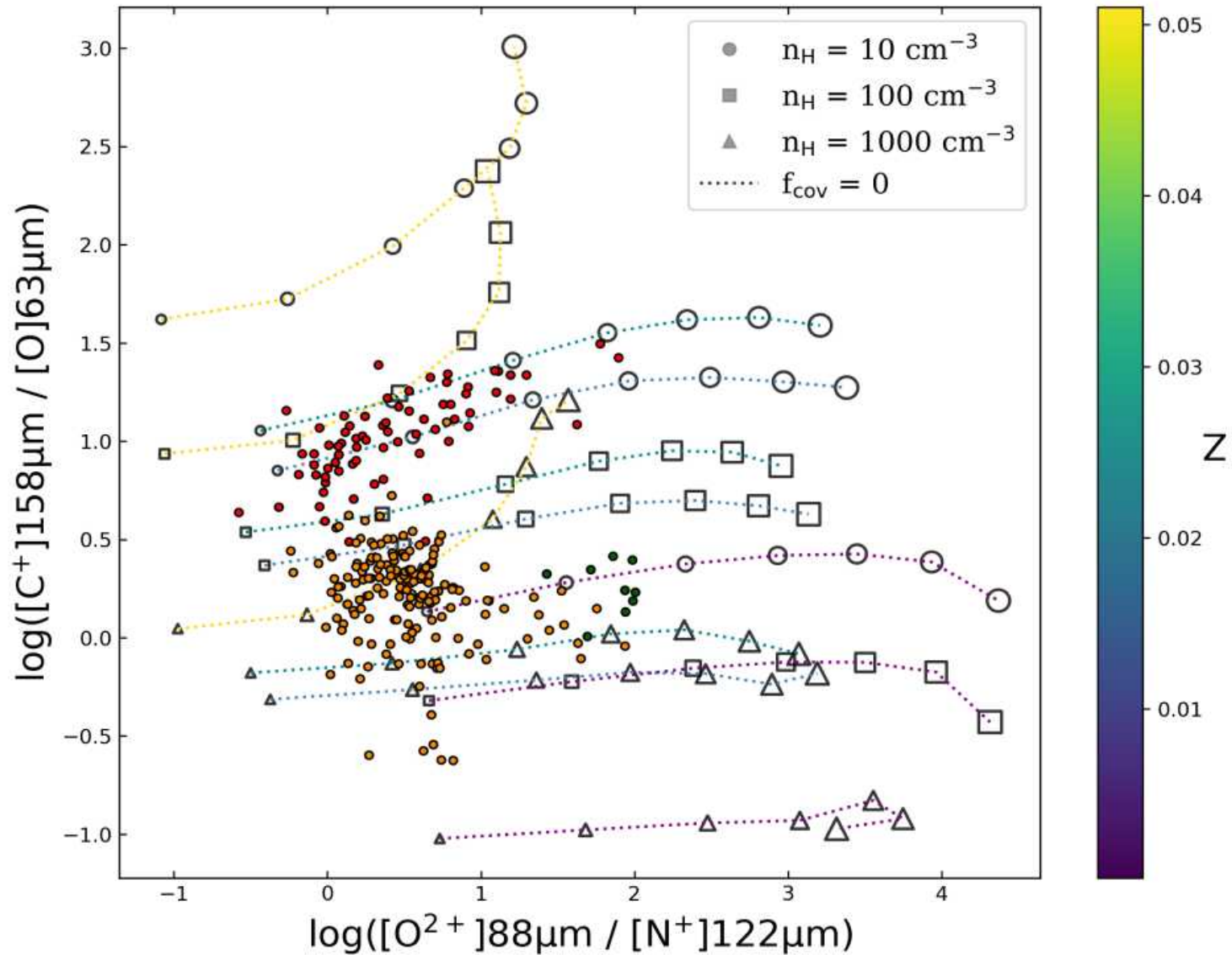
Tracers of the density n_H



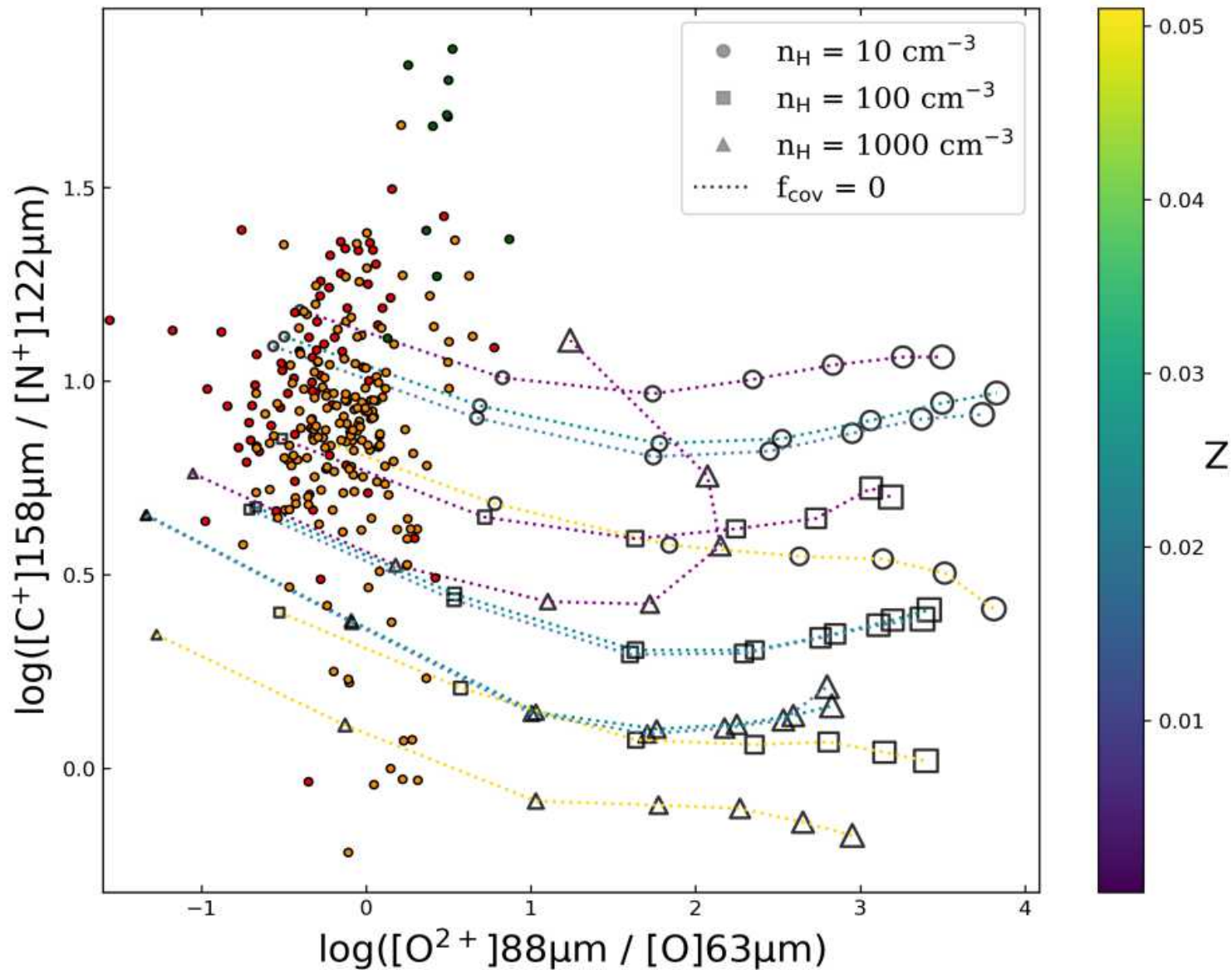
Tracers of the covering factor f_{cov}



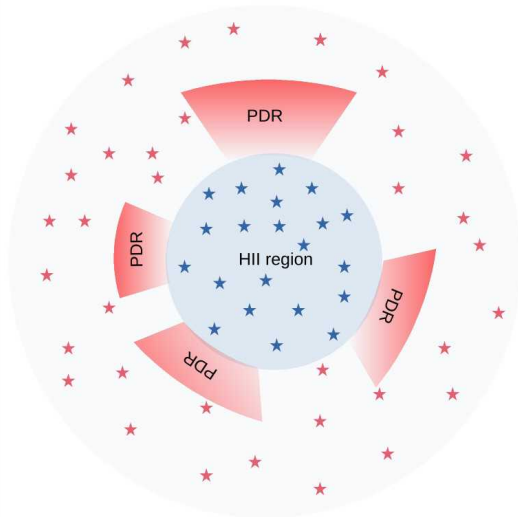
Infrared optical diagrams : the COON diagram



Infrared optical diagrams : the CNOO diagram



Starburst regions and photon dominated regions



Astronomy & Astrophysics manuscript no. IR_colors_lines_arXiv
November 11, 2022

©ESO 2022

Identification of Large Equivalent Width Dusty Galaxies at $4 < z < 6$ from Sub-mm Colours

D. Burgarella¹, P. Theulé¹, V. Buat¹, L. Gouiran¹, L. Turco¹, M. Boquien², T. J. L. C. Bakx^{3,4}, A. K. Inoue^{5,6}, Y. Fudamoto⁴, Y. Sugahara^{4,6}, and J. Zavala⁴

Astronomy & Astrophysics manuscript no. article_HIIPDR
June 12, 2023

©ESO 2023

Modeling the spectral energy distribution of starburst galaxies : the role of photodissociation regions

P. Theulé¹, D. Burgarella¹, V. Buat¹, M. Boquien², L. Trabelsi¹, and O. Kalpogiannis¹

¹ Aix Marseille Univ, CNRS, CNES, LAM, Marseille, France
e-mail: patrice.theule@lam.fr

² Centro de Astronomía (CITEVA), Universidad de Antofagasta, Avenida Angamos 601, Antofagasta, Chile

Received May 8, 2022; accepted March 16, 1997.

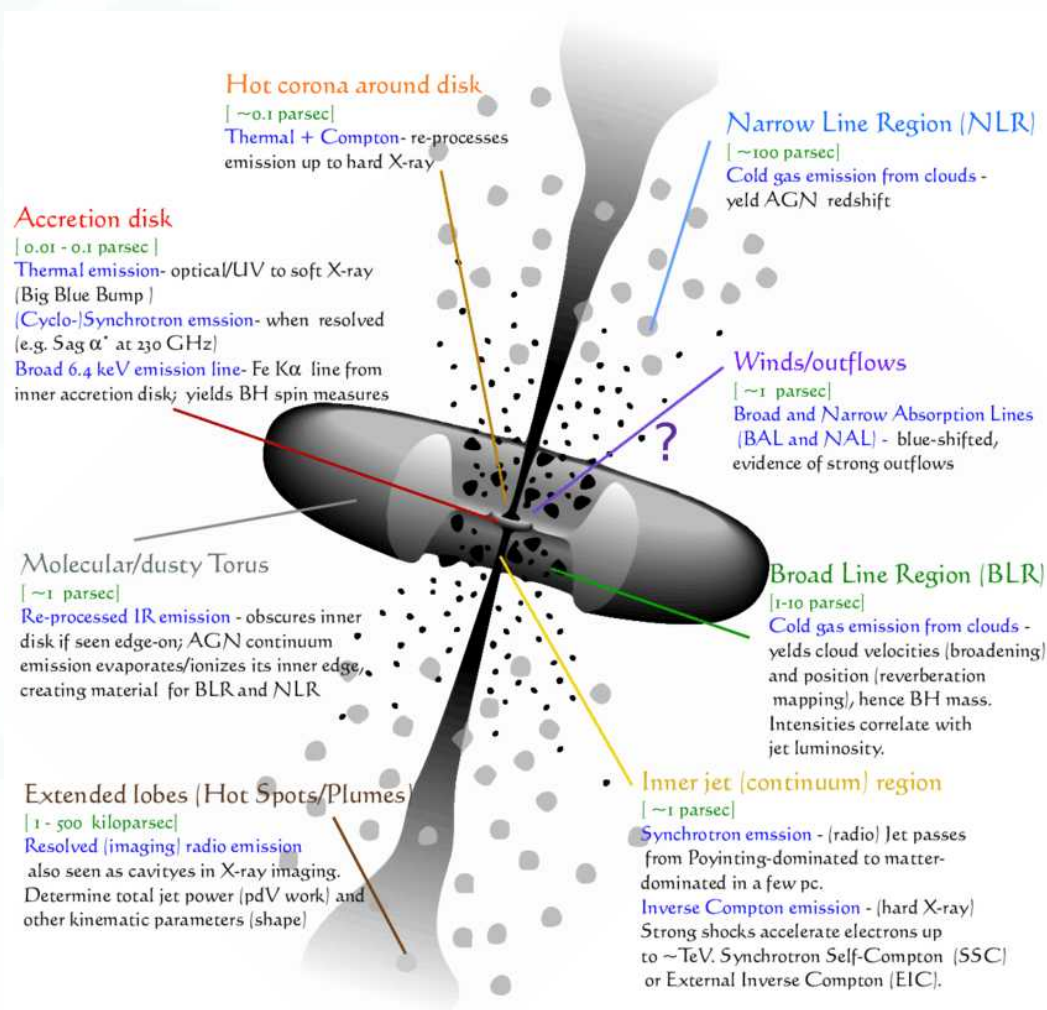
- useful diagnostic tracers
- strong correlation

→ new CIGALE module nebular_PDR

III. Active Galactic Nuclei hosting galaxies

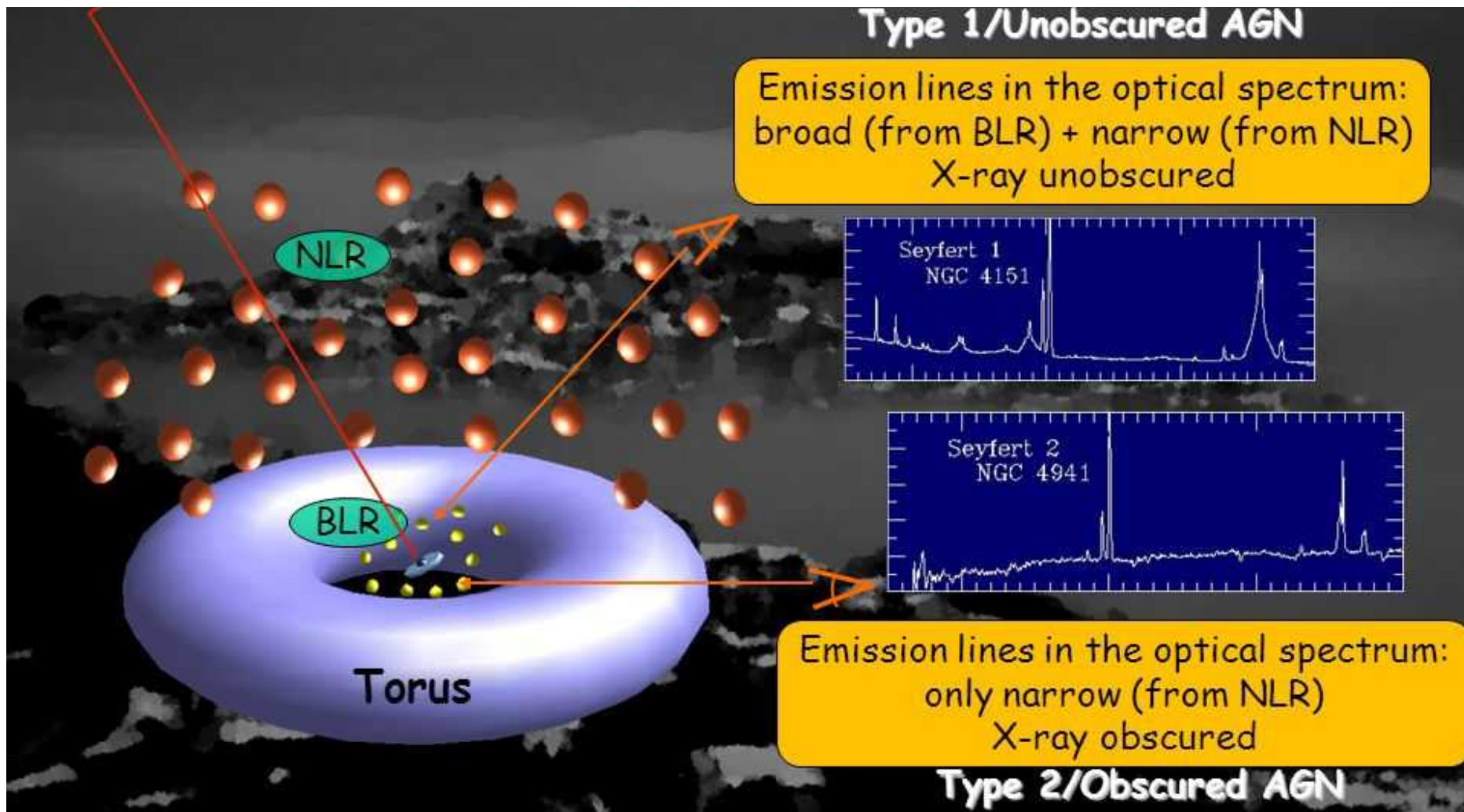


Anatomy of an Active Nuclei Galaxy



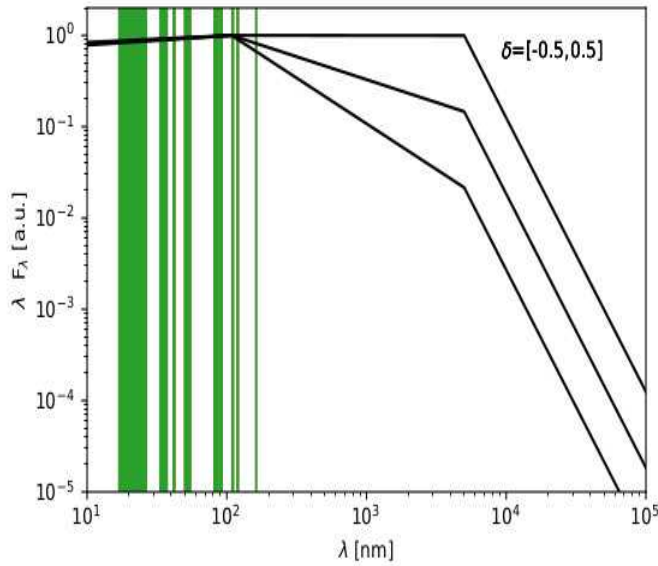
AGN spectra :

Narrow Line Regions (NLR) and Broad Line Regions (BLR)

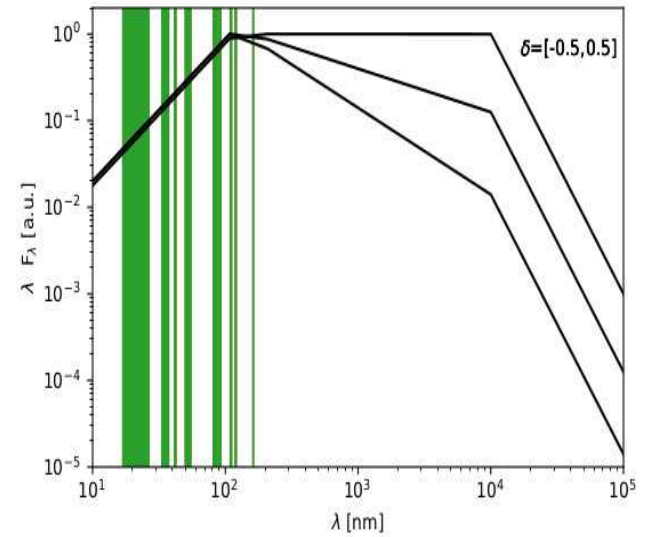


The accretion disk radiation field

SKIRTOR model



Schartmann model



champ
ionisant :
forme +
intensité

$\delta, \log U$

$$U \equiv \frac{Q(H)}{4\pi r_0^2 n(H)c} = \frac{N_{LyC}}{n(H)}$$

Dust and dust attenuation

dust has a role both on the chemistry (depletion, surface chemistry) and on the radiative transfer (diffusion / absorption)

NLR : standard depletion

NLR et BLR : SMC attenuation law (polar dust)

BLR : no depletion (all the grains are sublimated)

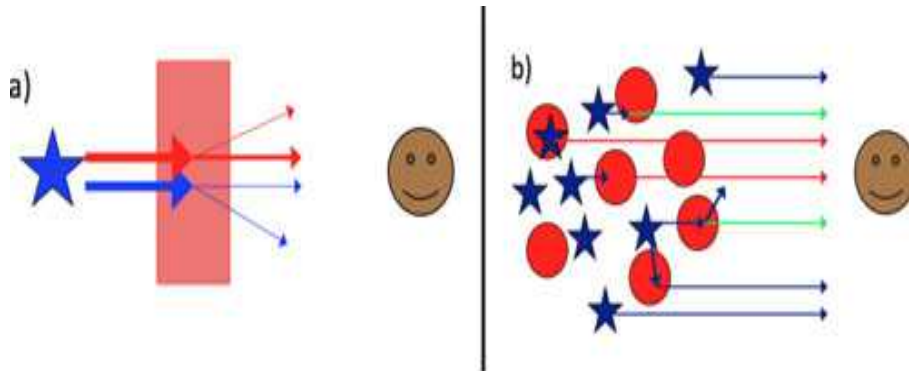
$$I = I_0 * 10^{\frac{-A_\lambda}{2.5}}$$

$$A_\lambda = E(B-V) * 1.39 \lambda_{\mu m}^{-1.2}$$

with $E(B-V) = 0.15$

extinction \neq attenuation

$$\frac{H\alpha}{H\beta} \quad \begin{array}{l} 656 \text{ nm} \\ 486 \text{ nm} \end{array}$$

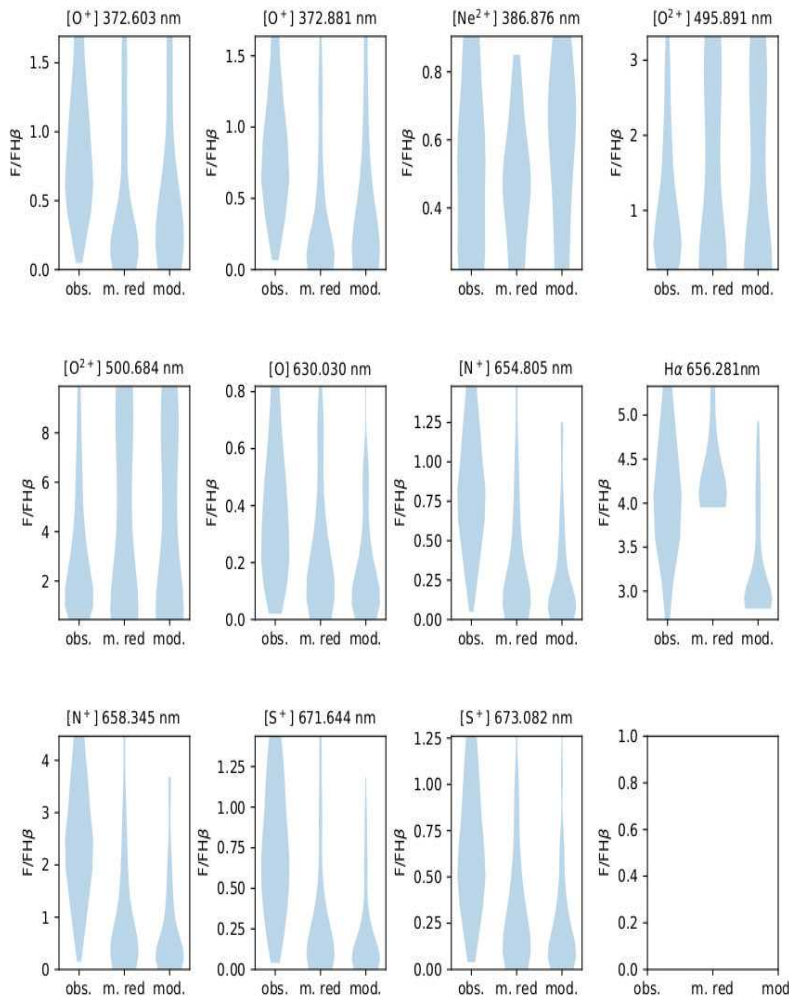


credit : D. Calzetti

Comparison models / observations

sample : 4XMM-DR9 x SDSS-DR12 catalogues (X source selection , 5σ)

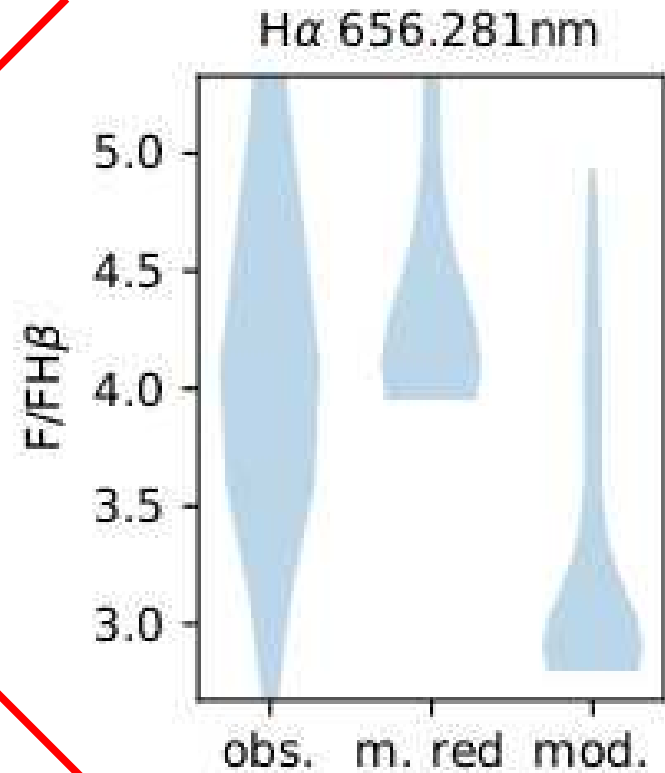
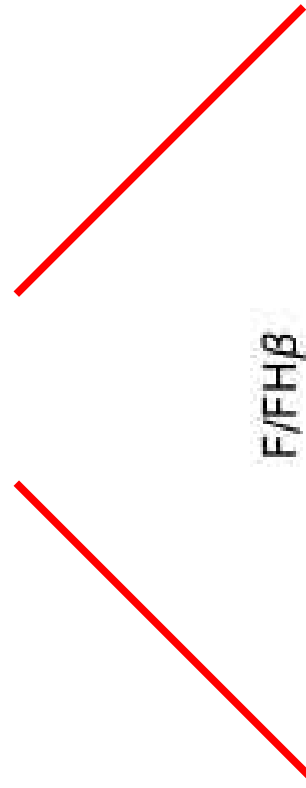
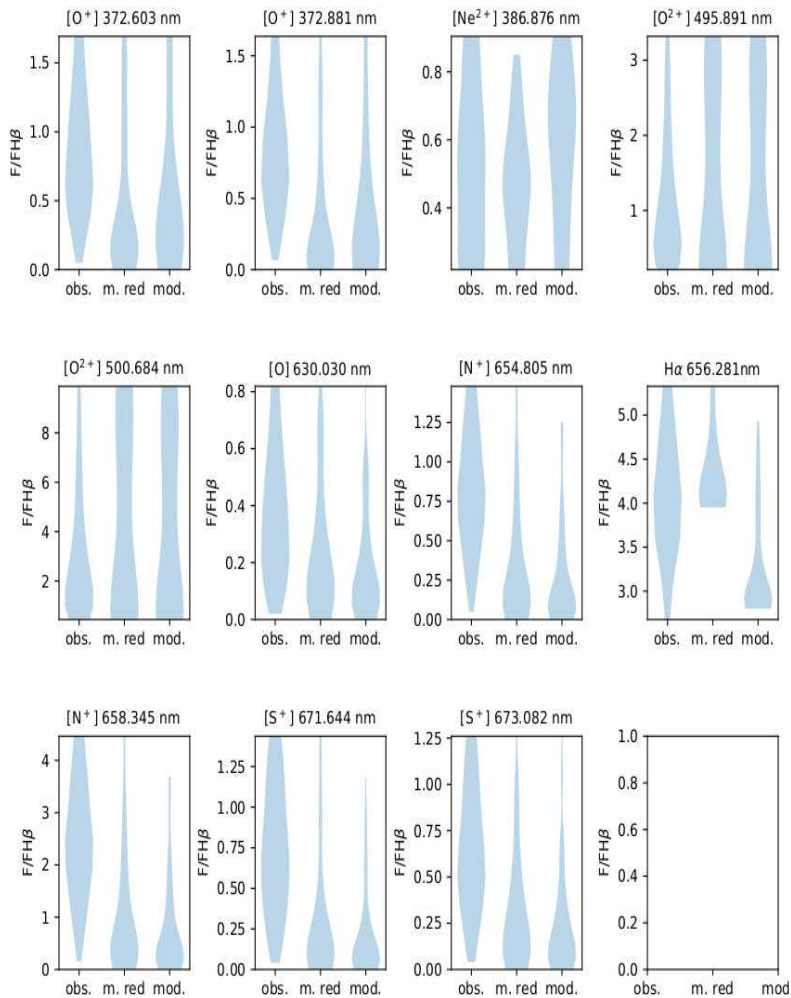
17 emission lines for NLRs , 3 lines for BLRs



Comparison models / observations

sample : 4XMM-DR9 x SDSS-DR12 catalogues (X source selection , 5σ)

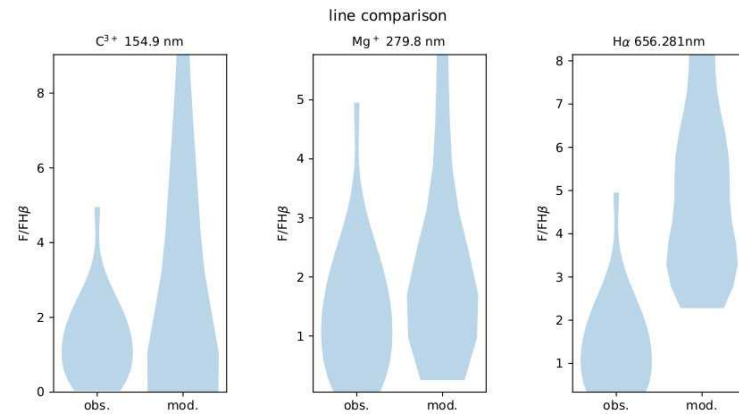
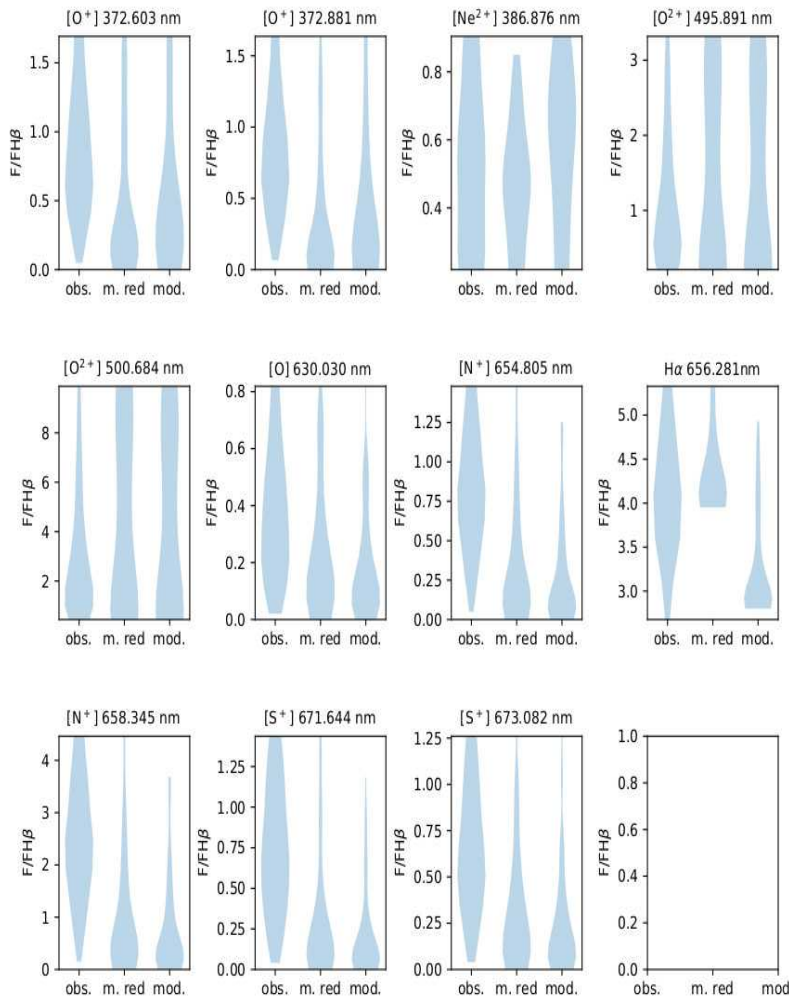
17 emission lines for NLRs , 3 lines for BLRs



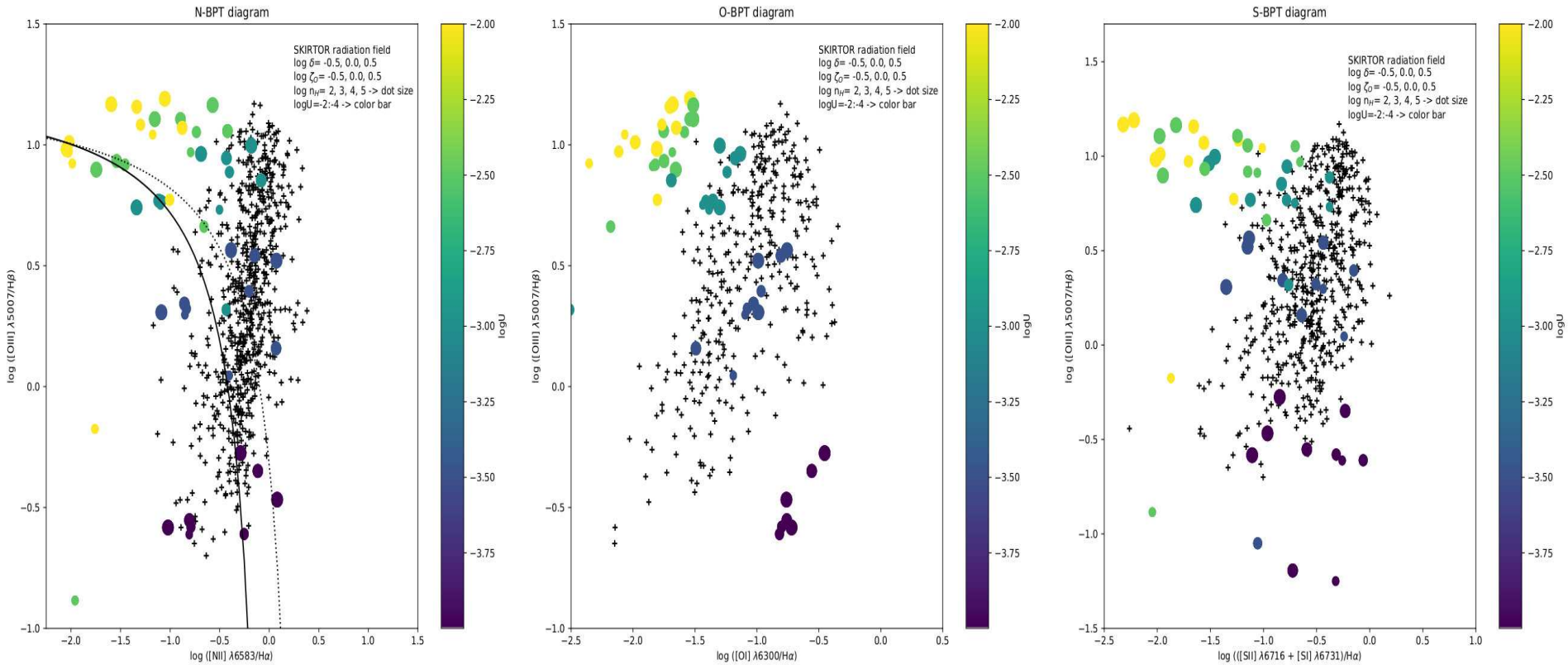
Comparison models / observations

sample : 4XMM-DR9 x SDSS-DR12 catalogues (X source selection , 5σ)

17 emission lines for NLRs , 3 lines for BLRs



Optical diagnostic diagrams



most of the observations are covered

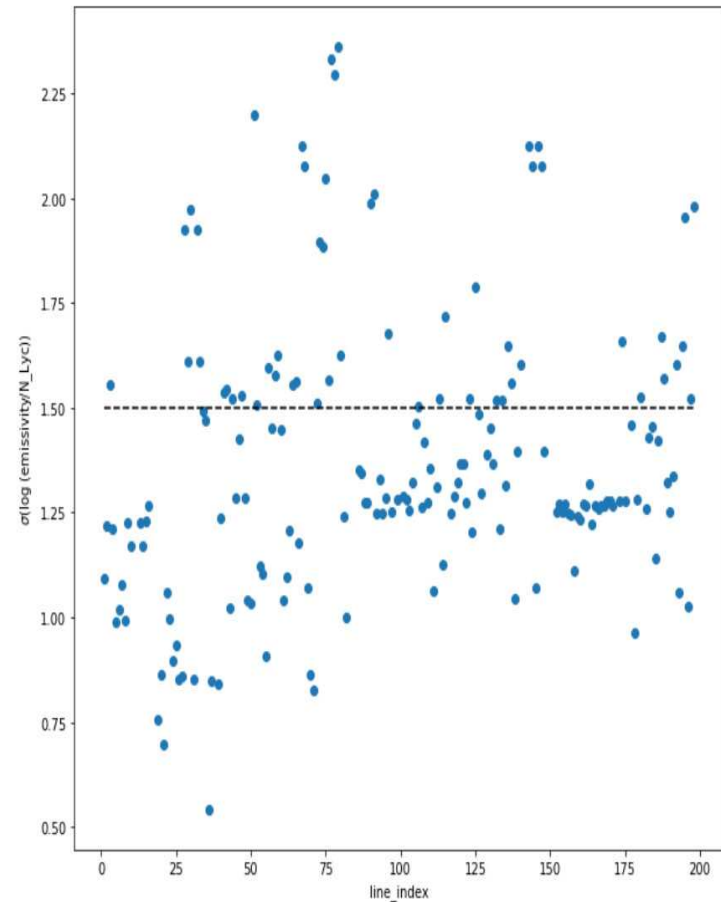
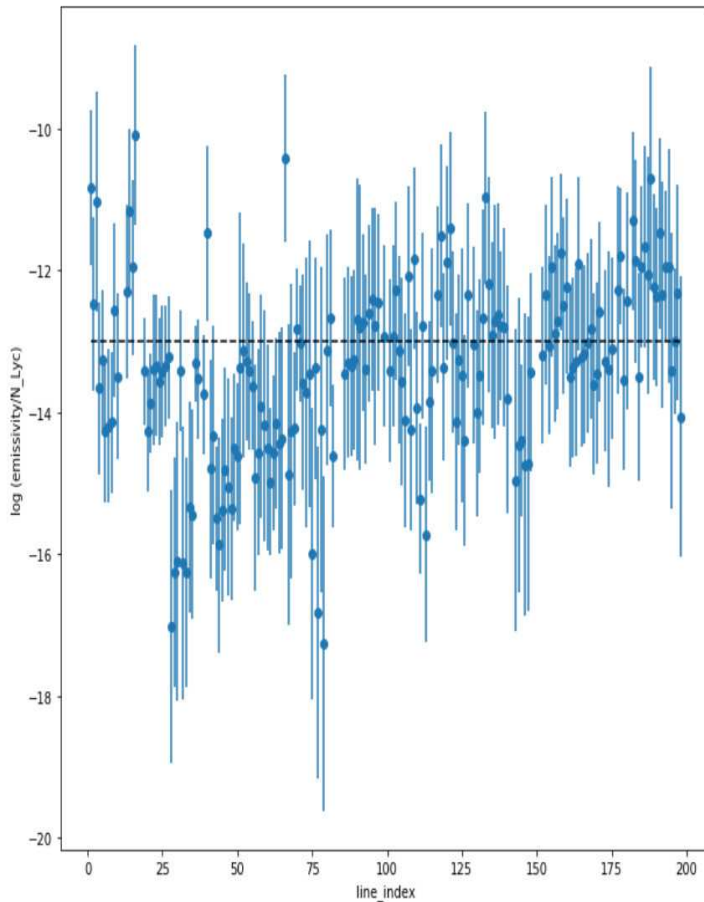
uncertainty on the elemental abundances

resulting degeneracy

Good spectroscopic diagnostics ?

good spectral diagnostic :

- strong intensity (observed)
- large variation as a function of one parameter



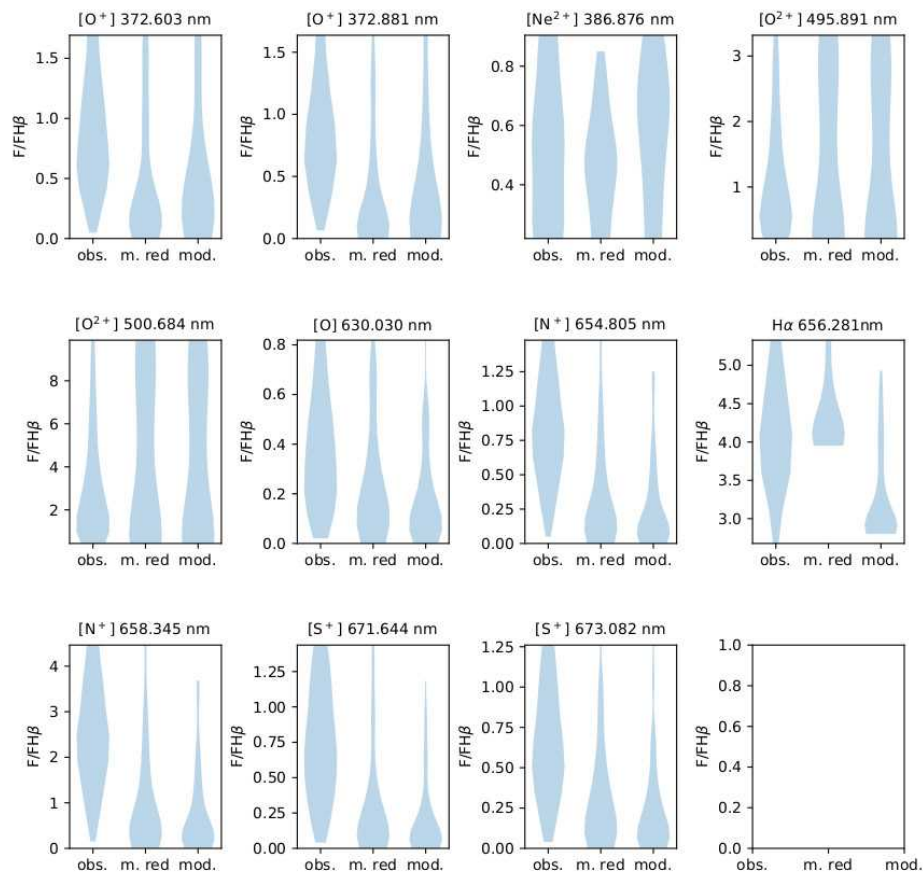
Good spectroscopic diagnostics ?

good spectral diagnostic :

- strong intensity (observed)
- large variation as a function of one parameter

line	δ	ζ_O	n_H	U
VUV-UV				
He 2 30.3784 nm			m	
He 1 62.5563 nm			m	s
H 1 121.567 nm			s	s
Si 4 139.375 / 140.277 nm	w			
C 4 154.819 nm (blend 154.9)	w			
He 2 164.043 nm			m	
O 3 166.615nm (blend 166.6 nm)	w			
Si 3 188.271 / 189.203 nm	w			
C 3 190.668 / .873 nm (blend 190.8)	w			
Ne 4 242.166 nm	w			
Ne 4 242.428 nm	w			
Ne 5 342.603 nm	w			
O 2 372.603/372.881 nm				m
visible				
O 3 436.321 nm	w			
H 1 486.133 nm				m
O 3 495.891 nm			m	
O 3 500.684 nm			s	
N 2 658.345 nm				m
S 3 953.062 nm				m
IR				
S 4 10.5076 μm			m	
N 3 15.5509 μm				m
S 2 18.7078 μm				m
O 4 25.8832 μm			m	
Fe 225.9811 μm				m
Si 2 34.8046 μm			m	s
O 3 51.8004 μm			m	

Active Galactic Nuclei hosting galaxies



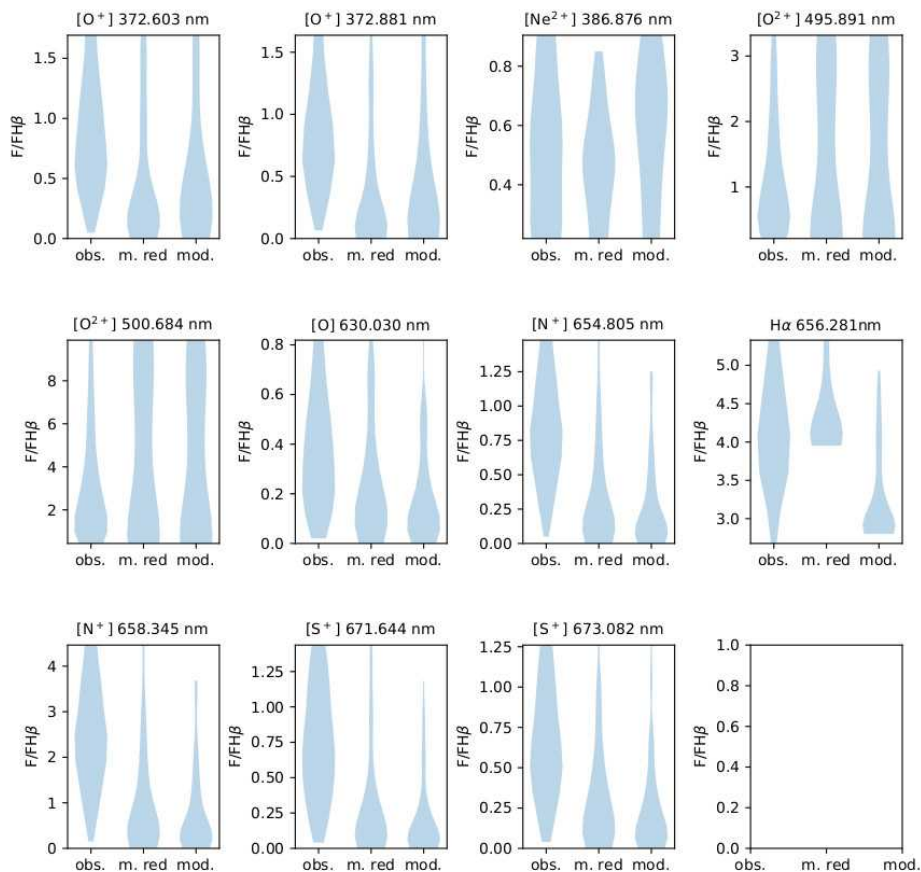
Theule et al. , 2024 in preparation

the ATHENA mission

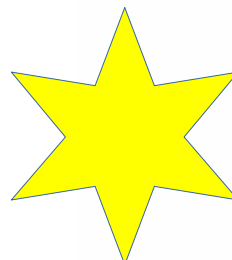


new module nebular_AGN

Active Galactic Nuclei hosting galaxies



Theule et al. , 2024 in preparation



open post-doc position
starting January 2024

the ATHENA mission



new module nebular_AGN



Thank you for your attention